J. Fluid Mech. (2009), *vol.* 633, *pp.* 327–353.
doi:10.1017/S0022112009006703 Printed in the United Kingdom

On inertial effects in the Moffatt–Pukhnachov coating-flow problem

MARK A. KELMANSON†

Department of Applied Mathematics, University of Leeds, Leeds LS2 9JT, UK

(Received 15 September 2008 and in revised form 26 February 2009)

The effects are investigated of including inertial terms, in both small- and large-surface-tension limits, in a remodelling of the influential and fundamental problem first formulated by Moffatt and Pukhnachov‡ in 1977: that of viscous thin-film free-surface Stokes flow exterior to a circular cylinder rotating about its horizontal axis in a vertical gravitational field.

An analysis of the non-dimensionalizations of previous related literature is made and the precise manner in which different rescalings lead to the asymptotic promotion or demotion of pure-inertial flux terms over gravitational-inertial terms is highlighted. An asymptotic mass-conserving evolution equation for a perturbed-film thickness is derived and solved using two-timescale asymptotics with a strained fast timescale. By using an algebraic manipulator to automate the asymptotics to high orders in the small expansion parameter of the ratio of the film thickness to the cylinder radius, consistent a posteriori truncations are obtained.

Via two-timescale and numerical solutions of the evolution equation, new light is shed on diverse effects of inertia in both small- and large-surface-tension limits, in each of which a critical Reynolds number is discovered above which the thin-film evolution equation has no steady-state solution due to the strength of the destabilizing inertial centrifugal force. Extensions of the theory to the treatment of thicker films are discussed.

1. Introduction

Almost a third of a century after its first consideration in Moffatt (1977) and Pukhnachev (1977), the evolution of viscous thin-film free-surface two-dimensional flow on the exterior of a rotating circular cylinder continues to stimulate interest on diverse theoretical and computational fronts, not least because of its industrial potential for modelling both coating and rimming flows, in which a thin film of viscous liquid with a free surface evolves respectively on the exterior and the interior of a circular cylinder rotating about its horizontal axis in a vertical gravitational field. Accordingly, although a considerable literature has emerged on both variants of the 'Moffatt–Pukhnachov' problem (MPP), and despite the attention it has received to date, the MPP continues to reveal new features at all levels, including the fundamental.

This paper concerns the new derivation of an explicit criterion, for the existence of a stable thin film in the exterior MPP, in terms of the three physical parameters describing the interplay between leading-order independent effects of gravity, surface

† Email address for correspondence: mark@maths.leeds.ac.uk

‡ The English transliteration Pukhnachev appears in only the original 1977 paper and reflects neither the correct pronunciation of the name in its original Cyrillic form nor its spelling in subsequent papers; it is used here only when citing the 1977 paper.

tension and inertia, by finding time-dependent asymptotic solutions of a newly derived inertial extension of the evolution equation of Pukhnachev (1977) for the height of the thin film.

Hinch & Kelmanson (2003) use two-timescale asymptotics to analyse the exterior MPP characterized by two non-dimensional parameters corresponding to gravity $\gamma = \rho g \bar{h}^2/3\omega\mu a$, and surface tension $\alpha = \sigma \bar{h}^3/3\omega\mu a^4$, where ω and a are respectively the angular velocity and radius of the cylinder, and μ, ρ, σ and $\bar{h}$ are respectively the dynamic viscosity, density, surface tension and mean film thickness of the fluid, and g is the gravitational acceleration. The low-harmonic analysis of Hinch & Kelmanson (2003) applies to the parameter hierarchy $\gamma^2 \ll \alpha \ll \gamma \ll 1$, and breaks down when $\alpha = O(\gamma^2)$. In the small-α régime, the modified asymptotic analysis of Hinch, Kelmanson & Metcalfe (2004) determines shock-like solutions by solving a Kuramoto–Sivashinsky evolution equation for the leading-order term in a γ-expansion of the film thickness. Hinch & Kelmanson (2003) theoretically confirm the numerical discovery of Hansen & Kelmanson (1994) that steady-state profiles are relatively insensitive to large variations in α, including those for which $\alpha \gg 1$, i.e. beyond the apparent validity of the above hierarchy.

The present paper extends the analysis of Hinch & Kelmanson (2003) by studying both theoretically and numerically the effect of augmenting Pukhnachov's equation by inertial terms proportional to a third non-dimensional parameter, a scaled Reynolds number $R = (\gamma\rho\sigma^3\bar{h}^{13}/81\alpha^3 g\mu^4 a^{13})^{1/2}$, which is thus fixed by the specification of γ and α, and whose position in the above hierarchy is therefore determined by the physical properties of a particular fluid.

Inertial corrections (to varying orders of accuracy) to the leading-order lubrication approximation have been incorporated in previous studies of rimming flow in, e.g., Benjamin, Pritchard & Tavener (1993), Hosoi & Mahadevan (1999), Acrivos & Jin (2004) and Benilov & O'Brien (2005). Noakes, King & Riley (2006) generalize the evolution-equation derivation of previous studies via a reconsideration of both exterior and interior MPPs using a systematic formal asymptotic approach, effectively deriving benchmark evolution equations for the purposes of comparison. Specifically, Noakes *et al.* (2006) incorporate inertial effects with emphasis on the modelling of generalized and consistent rational approximations of which the above studies, and this one, are specific limiting cases. Their formulation admits flexible velocity scalings, different parameter régimes, and uses a multiple-timescale approach to derive evolution equations for the leading-order components in a small-parameter expansion of the film profile; solving these equations is explicitly proposed as future work, and it is in this spirit that the present work is conducted, using mutually validating theoretical and numerical techniques.

Through a multiple-timescale study of our evolution equation, we discover that the interplay between leading-order gravity, surface tension and inertia gives rise to a critical Reynolds number below which centrifugal effects are dominated by surface tension, admitting a steady state, and above which centrifugal effects lead to oscillating growing solutions. A similar discovery is made by Hocking & Davis (2002) in an analysis of spreading drops, wherein a critical Reynolds number occurs below which the rate of approach to the steady state is reduced by inertia, but above which it becomes oscillatory; in the latter case, and in contrast to the present work, the absence of periodic gravitational forcing still admits a steady state.

The present work adheres to a fixed velocity scaling, retaining terms consistently by automating all calculations to high orders using the algebraic manipulator *Maple*, so that all truncations are controlled; in this sense, all expansions are calculated

to a far greater accuracy than can reasonably be presented herein. Since almost all of the derivations and calculations in §§2–5 require sophisticated non-trivial implementations in *Maple*, technical details are occasionally reported in order to convey both the intricacy and computational cost of the considerable quantity of otherwise-hidden details. The remainder of the paper is structured as follows.

In §2 an asymptotic mass-conserving evolution equation is derived, *ab initio* from the Navier–Stokes equations and boundary conditions, that augments the exterior-MPP Stokes-flow approximation of Pukhnachev (1977) with leading-order inertial effects. Apparent discrepancies between this evolution equation and those of related studies by Benjamin *et al.* (1993), Ashmore, Hosoi & Stone (2003) and Benilov & O'Brien (2005) are analysed in detail and fully explained by noting that the relative asymptotic ordering of what we classify as *pure-inertial* and *gravitational-inertial* effects is critically dependent upon the non-dimensionalization used. Leading-order gravitational, surface-tension and pure-inertial effects are respectively parameterized by the above-mentioned γ, α and R, and our equation (which is for a *perturbed normalized* film height, rather than the film height itself) is shown to be asymptotically consistent with the benchmark generalized theory of Noakes *et al.* (2006).

In §3 a two-timescale approach is used to solve the evolution equation derived in §2 as a power series in γ, using a strained fast timescale and a slow-timescale parameter γ^2 physically induced by the double action of gravity identified by Hinch & Kelmanson (2003); straining the fast timescale simplifies calculations by accommodating the drift element of the slow-timescale evolution equations at leading order; on this note, an explicit formula in terms of γ, α and R for the leading-order drift relative to the rotating cylinder is obtained. Since the introduction of inertia substantially increases the level of algebraic manipulation required to solve the γ-hierarchy of initial-boundary-value problems, automated and systematic bespoke *Maple* procedures are necessarily implemented in order to obtain all closed-form approximate solutions.

Using both the theoretical approximations of §3 and corroborative numerical simulations, inertial effects in the new model are investigated in §4. First, the two-timescale approximation contains terms that are unexpectedly singular (N.B. not secular) at certain integer-valued Weber numbers when $R = O(\alpha)$. In identifying the origin of such terms via wave-mode interactions, the discovery is made of an interesting artefact of the two-timescale solution: as $R \to 0$, certain source terms switch singularly from particular integrals into secularity conditions at each order of γ. This switching leads to a minute discrepancy, between two-timescale approximations obtained from $R \equiv 0$ and $R \to 0$, that decays exponentially with time. Second, the destabilizing centrifugal effect on the fundamental mode (of the exterior MPP) is quantified, leading to the discovery of a critical Reynolds number $R_0 = O(\alpha\gamma^2)$ above which inertia destabilizes the surface-tension-induced decay to the steady state analysed in previous related studies. The inertial stability threshold set by R_0 therefore precludes the attainment of the above-mentioned singular terms, so that the asymptotic solution remains uniformly valid on physical grounds.

Inertial perturbations to the steady state are studied in §5, with particular reference to the closed-form exact results of recent inertia-free studies by Pukhnachov (2005*a*, *b*) and Karabut (2007). It is discovered that the maximum-film-thickness location is shifted downwards (i.e. in the direction of gravity) by surface tension and inertia, and a formula for this location is obtained. As surface tension is increased to $\alpha \gg 1$, another critical Reynolds number, $R_\infty = O(\alpha^{-1})$, is found, and new large-α asymptotic formulae (with $R = R_\infty$) are shown to be in excellent agreement with recent theoretical

results (with $R=0$), even when the expansion parameter γ assumes unexpectedly large values of order $O(1)$.

2. Mass-conserving evolution equation

The evolution of a two-dimensional viscous capillary film on the exterior of a horizontal rotating cylinder is analysed in cylindrical-polar coordinates (r,θ) centred on the axis of the cylinder. With minor alterations, the present analysis is also applicable to the related problem on the interior of a rotating cylinder. The cylinder has radius a and rotates about its horizontal axis with constant angular velocity ω, and the fluid has dynamic viscosity, density and surface tension μ, ρ and σ, respectively; g is the acceleration due to gravity. Length, time, velocity, flux and pressure are respectively scaled by a, ω^{-1}, $a\omega$, $a^2\omega$ and $\rho a^2\omega^2$, and there are four non-dimensional parameters, three of which are the Reynolds, Galileo and Weber numbers, respectively given by

$$R_0=\frac{a^2\omega\rho}{\mu},\quad G_0=\frac{g}{a\omega^2}\quad\text{and}\quad W_0=\frac{\rho a^3\omega^2}{\sigma}. \tag{2.1}$$

If the dimensional film thickness is $\widetilde{h}(\theta,t)\ll a$, the fourth non-dimensional parameter is the ratio of the mean initial film thickness $\bar{h}$ and the cylinder radius,

$$\epsilon\equiv\frac{1}{2\pi a}\int_{\theta=0}^{2\pi}\widetilde{h}(\theta,0)\,d\theta=\frac{\bar{h}}{a} \tag{2.2}$$

which, satisfying $0<\epsilon\ll 1$, constitutes the expansion parameter in the subsequent asymptotic analysis. Define dimensionless rescaled parameters by

$$\lambda_{PUK}=\epsilon^2G_0R_0,\quad \chi_{PUK}=\epsilon^3\frac{R_0}{W_0}\quad\text{and}\quad \Phi_{PUK}=\epsilon^2R_0, \tag{2.3}$$

and a dimensionless, rescaled film height $H(\theta,t)$ by

$$\widetilde{h}(\theta,t)=a\epsilon H(\theta,t) \tag{2.4}$$

so that, by (2.2) and (2.4), $H(\theta,0)$ has unit mean in $[0,2\pi]$. Pukhnachev (1977) derives an *asymptotic* evolution equation for $H(\theta,t)$,

$$H_t+\left\{H-\tfrac{1}{3}\lambda_{PUK}H^3\cos\theta+\tfrac{1}{3}\chi_{PUK}H^3(H_\theta+H_{\theta\theta\theta})\right\}_\theta=0, \tag{2.5}$$

by postulating that, in the limit $\epsilon\to 0$, parameters λ_{PUK}, χ_{PUK} and Φ_{PUK} approach finite values, the last of which is chosen to be zero. As shown below, the alternative rescaling of ϵ^3R_0 is required to incorporate leading inertial effects consistently in (2.5), which is therefore automatically asymptotically correct – i.e. without imposing the choice $\Phi_{PUK}=0$ – simply by virtue of the last scaling in (2.3). However, as shown below, (2.5) does not conserve mass, but it can be interpreted to do so through a simple perturbation in the definition of H.

If r, u, v and p are respectively the dimensionless radial coordinate, radial velocity, tangential velocity and pressure, and if $h=\widetilde{h}/a$ is the order $O(\epsilon)$ dimensionless film thickness, the Navier–Stokes equations are

$$u_t+uu_r+\frac{vu_\theta}{r}-\frac{v^2}{r}=-p_r+\frac{1}{R_0}\left(u_{rr}+\frac{u_r}{r}+\frac{u_{\theta\theta}}{r^2}-\frac{2v_\theta}{r^2}-\frac{u}{r^2}\right)-G_0\sin\theta, \tag{2.6}$$

$$v_t + uv_r + \frac{vv_\theta}{r} + \frac{uv}{r} = -\frac{p_\theta}{r} + \frac{1}{R_0}\left(v_{rr} + \frac{v_r}{r} + \frac{v_{\theta\theta}}{r^2} + \frac{2u_\theta}{r^2} - \frac{v}{r^2}\right) - G_0\cos\theta, \quad (2.7)$$

$$(ru)_r + v_\theta = 0, \quad (2.8)$$

in the annulus $1 < r < 1+h$, $0 \leqslant \theta \leqslant 2\pi$, for $t \geqslant 0$. The no-slip condition on the cylinder at $r = 1$ is

$$u = 0, \quad v = 1, \quad (2.9)$$

and the kinematic, shear-stress and normal-stress conditions on the free surface at $r = 1 + h$ are respectively

$$h_t + \frac{v}{r}h_\theta - u = 0, \quad (2.10)$$

$$\left(1 - \frac{h_\theta^2}{r^2}\right)\left(v_r - \frac{v}{r} + \frac{u_\theta}{r}\right) + \frac{2h_\theta}{r}\left(u_r - \frac{u}{r} - \frac{v_\theta}{r}\right) = 0, \quad (2.11)$$

$$-p + 2\frac{u_r - (h_\theta/r^2)(rv_r - v + u_\theta) + \left(h_\theta^2/r^3\right)(u + v_\theta)}{R_0\left(1 + \left(h_\theta^2/r^2\right)\right)} = \frac{\kappa}{W_0}, \quad (2.12)$$

in which the free-surface curvature is

$$\kappa = -\frac{(1+h)^2 + 2h_\theta^2 - (1+h)h_{\theta\theta}}{\left((1+h)^2 + h_\theta^2\right)^{3/2}}. \quad (2.13)$$

Using the algebraic manipulator *Maple*, a fully automated solution procedure has been implemented, in terms of power series in ϵ, for the boundary-and-initial-value problem (2.6)–(2.13). As the details are rather cumbersome, only a summary of the solution strategy and key observations is presented. The thin-film scalings in Pukhnachev (1977) are introduced for the 2π-periodic functions h, u, v and p,

$$r = 1 + \epsilon Y, \quad u = \epsilon U, \quad v = V \quad \text{and} \quad p = P,$$

which supplement (2.4) and in which the functions U, V and P having $O(1)$ moduli are expanded as the series

$$\begin{Bmatrix} U \\ V \\ P \end{Bmatrix} = \sum_{k=0}^{N} \epsilon^k \begin{Bmatrix} U^{(k)} \\ V^{(k)} \\ P^{(k)} \end{Bmatrix} (Y, \theta, t),$$

for some preselected N. At each order $O(\epsilon^k)$, $k = 0, \ldots, N$, $V_{YY}^{(k)}$ is first isolated in (2.7) and $V^{(k)}$ is determined via boundary conditions (2.9) and (2.11). With $V^{(k)}$ known, $U_Y^{(k)}$ is then isolated in (2.8) and $U^{(k)}$ is determined via boundary condition (2.9). Using $U^{(k)}$ and $V^{(k)}$, $P_Y^{(k)}$ is finally isolated in (2.6) and determined via boundary condition (2.12). The automation is swift: on a Dell laptop with a 2.4 GHz Pentium 4 processor and 512Mb RAM running *Maple 9.0* on Windows XP, the CPU times (in seconds) taken to solve $U^{(k)}$, $V^{(k)}$ and $P^{(k)}$ for $k = 0, \ldots, N = 7$ were 0.03, 0.05, 0.09, 0.19, 0.35, 1.06, 4.54 and 20.88, respectively. The flux is obtained from

$$Q = \int_0^H V(Y)\,\mathrm{d}Y$$

in which, through (2.6) and (2.7), H_t and H_{tt} occur at orders $O(\epsilon^4)$ and $O(\epsilon^6)$ respectively. The kinematic free-surface condition (2.10) is now used to remove H_t from Q – more precisely to telescope it iteratively beyond $O(\epsilon^N)$ in Q – and then

H_{tt} is similarly telescoped further into Q using the temporal derivative of (2.10) augmented by $U_t(H,\theta,t)$ and $V_t(H,\theta,t)$. For $N=7$, the automated computation of Q and telescoping process requires only a single iteration and takes a further 34.28 s, yielding

$$\begin{aligned} Q = {} & H + \tfrac{1}{2}\epsilon H^2 - \tfrac{1}{3}\gamma_0\epsilon^2 H^3\cos\theta \\ & + \epsilon^3\left\{\tfrac{1}{3}\alpha_0 H^3(H_\theta + H_{\theta\theta\theta}) + \tfrac{1}{3}R_0 H^3 H_\theta - \gamma_0\left[\tfrac{1}{3}H^3 H_\theta\sin\theta + \tfrac{1}{2}H^4\cos\theta\right]\right\} \\ & + \epsilon^4\left\{\gamma_0\left[\tfrac{9}{20}H^5\cos\theta + \tfrac{17}{6}H^4 H_\theta\sin\theta - H^4 H_{\theta\theta}\cos\theta - \tfrac{7}{3}H^3 H_\theta^2\cos\theta\right]\right. \\ & \left. - \alpha_0\left[\tfrac{1}{2}H^4(H_\theta + H_{\theta\theta\theta}) + H^3 H_\theta H_{\theta\theta}\right] + \tfrac{1}{2}R_0 H^4 H_\theta - \tfrac{2}{15}\gamma_0 R_0 H^5\sin\theta\right\} \\ & + O(\epsilon^5) \end{aligned} \tag{2.14}$$

in which R_0 is given by (2.1) and γ_0 and α_0 respectively by

$$\gamma_0 = \frac{a\rho g}{\omega\mu} \quad \text{and} \quad \alpha_0 = \frac{\sigma}{a\omega\mu}. \tag{2.15}$$

An advantage of using the kinematic free-surface condition iteratively to telescope temporal derivatives to higher orders of ϵ is the explicit determination of Q in terms of H and its derivatives with respect to θ only, so that (2.14) can be used directly to construct an evolution equation with a prespecified truncation error, here $O(\epsilon^8)$ and higher. The order $O(\epsilon^n)$ terms in (2.14) for $n=5,6,7$ are explicitly known but too cumbersome to present.

Differences in Q born of different non-dimensionalizations are now discussed, present interest being focused on the potential promotion or demotion of inertial terms in rescaled small-parameter expansions of Q. Distinguished by their parametric factors in (2.14), we subsequently refer to $(1/3)\epsilon^3 R_0 H^3 H_\theta$ and $(1/2)\epsilon^4 R_0 H^4 H_\theta$ as pure-inertial (PI) terms, and to $-(2/15)\epsilon^4\gamma_0 R_0 H^5\sin\theta$ as a gravitational-inertial (GI) term. Benjamin *et al.* (1993) define $\alpha_{BPT} = (\omega\mu/\rho g a)^{1/2}$ to be their small parameter. Then $\alpha_{BPT} = 1/\sqrt{\gamma_0}$ and $B = \alpha_0/\gamma_0$ is the inverse Bond number, and the rescaling $H = \alpha_{BPT}\overline{H}/\epsilon$ transforms (2.14) into

$$\begin{aligned} Q_{BPT} = {} & \overline{H} - \tfrac{1}{3}\overline{H}^3\cos\theta + \alpha_{BPT}\left\{\tfrac{1}{2}\overline{H}^2 - \tfrac{1}{2}\overline{H}^4\cos\theta - \tfrac{1}{3}\overline{H}^3\overline{H}_\theta\sin\theta + \tfrac{1}{3}B\overline{H}^3(\overline{H}_\theta + \overline{H}_{\theta\theta\theta})\right\} \\ & + \alpha_{BPT}^2\left\{\tfrac{9}{20}\overline{H}^5\cos\theta + \tfrac{17}{6}\overline{H}^4\overline{H}_\theta\sin\theta - \overline{H}^4\overline{H}_{\theta\theta}\cos\theta - \tfrac{7}{3}\overline{H}^3\overline{H}_\theta^2\cos\theta\right. \\ & - B\left[\tfrac{1}{2}\overline{H}^4(\overline{H}_\theta + \overline{H}_{\theta\theta\theta}) + \overline{H}^3\overline{H}_\theta\overline{H}_{\theta\theta}\right] \\ & \left. + R_0\left[\tfrac{2}{15}\overline{H}^6\overline{H}_\theta\cos^2\theta - \tfrac{2}{15}\overline{H}^5\sin\theta - \tfrac{4}{315}\overline{H}^7\sin 2\theta\right]\right\} + O\left(\alpha_{BPT}^3\right). \end{aligned} \tag{2.16}$$

The first line of (2.16) constitutes a slight modification of Benjamin *et al.* (1993, (30)). This scaling binds leading-order gravitational effects to the leading-order viscous effect, with hydrostatic and capillary effects appearing at first order and inertial effects at second order.

A comparison of expansions (2.14) and (2.16) reveals that it is the inertial terms that undergo the most pronounced scaling-dependent promotion and demotion, as heralded by the factor H^3 in the first appearance of R_0 in (2.14) but $\overline{H}^5$, $\overline{H}^6$ and $\overline{H}^7$ in (2.16). Only one GI term, $-(2/15)\epsilon^4\gamma_0 R_0 H^5\sin\theta$ in Q and $-(2/15)\alpha_{BPT}^2 R_0\overline{H}^5\sin\theta$ in Q_{BPT}, is common to both expansions to the orders presented. Inspection of higher-order terms not explicitly presented in (2.14) and (2.16) reveals that the PI terms $(1/3)\epsilon^3 R_0 H^3 H_\theta$ and $(1/2)\epsilon^4 R_0 H^4 H_\theta$ in Q are

respectively demoted to $(1/3)\alpha_{BPT}^3 R_0 \overline{H}^3 \overline{H}_\theta$ and $(1/2)\alpha_{BPT}^4 R_0 \overline{H}^4 \overline{H}_\theta$ in Q_{BPT}, whereas the GI terms $(2/15)\epsilon^6\gamma_0^2 R_0 H^6 H_\theta \cos^2\theta$ and $-(4/315)\epsilon^6\gamma_0^2 R_0 H^7 \sin 2\theta$ in Q are respectively promoted to $(2/15)\alpha_{BPT}^2 R_0 \overline{H}^6 \overline{H}_\theta \cos^2\theta$ and $-(4/315)\alpha_{BPT}^2 R_0 \overline{H}^7 \sin 2\theta$ in Q_{BPT}.

Benilov & O'Brien (2005) promote the GI terms in (2.16) to the same order as hydrostatic and capillary terms by using the small parameter $\epsilon_{BO} = \alpha_{BPT}$ that multiplies the hydrostatic pressure to rescale inertial and capillary parameters as $\alpha_{BO} = \epsilon_{BO}^2 R_0$ and $\beta_{BO} = \epsilon_{BO} B$. Translated into the present notation, and with its sign reversed for the exterior MPP, their film height (Benilov & O'Brien 2005, (2)) is transformed via the (implicit) rescaling $H + (1/2)\epsilon H^2 = \epsilon_{BO}\widehat{H}/\epsilon$. Presently solving this for $H(\widehat{H})$ by series reversion, (2.14) becomes

$$\begin{aligned} Q_{BO} = {} & \widehat{H} - \tfrac{1}{3}\widehat{H}^3\cos\theta - \tfrac{1}{3}\epsilon_{BO}\widehat{H}^3\widehat{H}_\theta \sin\theta + \tfrac{1}{3}\beta_{BO}\widehat{H}^3(\widehat{H}_\theta + \widehat{H}_{\theta\theta\theta}) \\ & + \alpha_{BO}\left[\tfrac{2}{15}\widehat{H}^6\widehat{H}_\theta\cos^2\theta - \tfrac{2}{15}\widehat{H}^5\sin\theta - \tfrac{4}{315}\widehat{H}^7\sin 2\theta\right] + \mathscr{T}_{BO}, \end{aligned} \tag{2.17}$$

in which the truncation error $\mathscr{T}_{BO}$ is to leading order a linear combination of five of the six possible quadratic products (β_{BO}^2 is absent) of ϵ_{BO}, β_{BO} and α_{BO}. But for a slight modification (2.17) without the term $\mathscr{T}_{BO}$ is the flux implicit in Benilov & O'Brien (2005, (3)). Because of the iterative telescoping of temporal derivatives used in deriving Q, the 26 terms in $\mathscr{T}_{BO}$ are known explicitly, one of them being $(1/3)\epsilon_{BO}\alpha_{BO}\widehat{H}^3\widehat{H}_\theta$, which identifies with a demotion of the leading-order PI term $(1/3)\epsilon^3 R_0 H^3 H_\theta$ in Q.

Ashmore *et al.* (2003) consider the stationary interior-MPP problem using the filling fraction A as the small parameter, with corresponding gravitational and capillary parameters $\lambda_{AHS} = A/\gamma_0^2$ and $\mathscr{B} = A\alpha_0/\gamma_0$ respectively. The rescaling $H = A\widetilde{H}/\epsilon$ transforms the flux (2.14) into

$$\begin{aligned} Q_{AHS} = {} & \widetilde{H} - \tfrac{1}{3}\lambda_{AHS}\widetilde{H}^3\cos\theta + \tfrac{1}{3}\lambda_{AHS}\mathscr{B}\widetilde{H}^3(\widetilde{H}_\theta + \widetilde{H}_{\theta\theta\theta}) + A\big\{\tfrac{1}{2}\widetilde{H}^2 - \tfrac{1}{2}\lambda_{AHS}\widetilde{H}^4\cos\theta \\ & - \tfrac{1}{3}\lambda_{AHS}\widetilde{H}^3\widetilde{H}_\theta\sin\theta - \tfrac{1}{2}\lambda_{AHS}\mathscr{B}\widetilde{H}^4(\widetilde{H}_\theta + \widetilde{H}_{\theta\theta\theta}) - \lambda_{AHS}\mathscr{B}\widetilde{H}^3\widetilde{H}_\theta\widetilde{H}_{\theta\theta}\big\} \\ & + A^2\lambda_{AHS}\mathscr{T}_{AHS}, \end{aligned} \tag{2.18}$$

which corresponds to Ashmore *et al.* (2003, (2.13)), with which (2.18) now has more than the expected differences. In this case additional discrepancies at order $O(A)$ arise because Ashmore *et al.* (2003) approximate the exact curvature (2.13) as a series expansion in A. The truncation error in (2.18), in which $\mathscr{T}_{AHS} = O(\mathscr{B}, R_0, \lambda_{AHS}R_0, \lambda_{AHS}\mathscr{B}R_0)$, includes the leading GI terms of (2.16) and (2.17) over two orders, $O(A^2\lambda_{AHS}R_0)$ and $O(A^2\lambda_{AHS}^2 R_0)$, and the leading PI term of (2.14) at order $O(A^3R_0)$. In contrast to Q_{BPT} and Q_{BO}, and in common with Q, the leading-order gravitational term in Q_{AHS} may be varied independently of the leading-order viscous term.

The above comparisons clearly demonstrate that the relative asymptotic ordering of PI and GI terms in previous related studies is markedly affected by the non-dimensionalization used, and may accordingly influence conclusions. For example, for the interior MPP, Noakes *et al.* (2006, p. 176) comment that their (centrifugal) PI term stabilizes the fundamental mode, whereas the GI terms in Benilov & O'Brien (2005) always cause instability. The contradiction is only apparent, and is explained by noting that PI terms originate from inertial components of the radial Navier–Stokes equation (2.6) whereas GI terms do so from the interaction between inertial and gravitational components of the azimuthal Navier–Stokes equation (2.7). Under the present scaling, PI and GI terms are respectively of first and second order, and hence the asymptotic evolution equation now derived will contain only the former.

The dimensionless equation of mass conservation obtained from (2.8) and (2.10) is

$$(1+\epsilon H)H_t + Q_\theta = 0, \tag{2.19}$$

the first term of which is the temporal derivative of the sum of the first two terms on the right-hand side of (2.14), suggesting the introduction of a perturbed height

$$\mathscr{H}(\theta,t) = \frac{H(\theta,t)+(1/2)\epsilon H(\theta,t)^2}{1+(1/2)\epsilon H(\theta,0)} \tag{2.20}$$

which has been normalized to have the initial condition $\mathscr{H}(\theta,0)=H(\theta,0)$. The numerator of (2.20) translates to the exterior-MPP counterpart of Benilov & O'Brien (2005, (2)) used in the derivation of Q_{BO} in (2.17). To simplify the subsequent analysis, attention is restricted to the uniform initial condition $H(\theta,0)=1$, as detailed algebraic digressions indicate that certain initial conditions may considerably complicate the solution procedure of § 3 independently of the inertial effects with which this paper is concerned. With $H(\theta,0)=1$, inversion of (2.20) gives

$$\begin{aligned} H = \mathscr{H} &- \tfrac{1}{2}\epsilon\mathscr{H}(\mathscr{H}-1) + \tfrac{1}{2}\epsilon^2\mathscr{H}^2(\mathscr{H}-1) \\ &- \tfrac{1}{8}\epsilon^3\mathscr{H}^2(\mathscr{H}-1)(5\mathscr{H}-1) + \tfrac{1}{8}\epsilon^4\mathscr{H}^3(\mathscr{H}-1)(7\mathscr{H}-3) + O(\epsilon^5), \end{aligned} \tag{2.21}$$

which is substituted into a *perturbed flux* defined by $\mathscr{Q}=Q/(1+(1/2)\epsilon)$ to give

$$\begin{aligned} \mathscr{Q} = \mathscr{H} &- \tfrac{1}{3}\epsilon^2\gamma_0\mathscr{H}^3\cos\theta \\ &+ \tfrac{1}{3}\epsilon^3\mathscr{H}^3\{\alpha_0(\mathscr{H}_\theta + \mathscr{H}_{\theta\theta\theta}) - \gamma_0(\cos\theta + \mathscr{H}_\theta\sin\theta) + R_0\mathscr{H}_\theta\} + O(\epsilon^4), \end{aligned} \tag{2.22}$$

in which terms of order $O(\epsilon^n)$ for $n=4,5,6,7$ are known but not presented. Equations (2.19)–(2.22) yield the evolution equation for $\mathscr{H}$ as

$$\mathscr{H}_t + \mathscr{Q}_\theta = 0, \tag{2.23}$$

which is mass-conserving to order $O(\epsilon^7)$ whereas (2.5) is so only to order $O(1)$.

Motivated by the leading-order appearances of gravitational, capillary and pure-inertial terms in (2.14), introduce the scalings

$$\gamma = \tfrac{1}{3}\epsilon^2\gamma_0, \quad \alpha = \tfrac{1}{3}\epsilon^3\alpha_0 \quad \text{and} \quad R = \tfrac{1}{3}\epsilon^3 R_0, \tag{2.24}$$

in which: γ and α (cf. Hinch & Kelmanson 2003, (2.10)) are respectively renormalized versions of λ_{PUK} and χ_{PUK} (cf. Pukhnachev 1977) in (2.3); R is an order of magnitude smaller than the inertial coefficient Φ_{PUK} in (2.3), and $\gamma,\alpha,R \ll 1$ when $\gamma_0,\alpha_0,R_0=O(1)$. Via the scalings (2.24), the normalized flux (2.22) becomes

$$\mathscr{Q} = \mathscr{H} - \gamma\mathscr{H}^3\cos\theta + \alpha\mathscr{H}^3(\mathscr{H}_\theta + \mathscr{H}_{\theta\theta\theta}) + R\mathscr{H}^3\mathscr{H}_\theta + \mathscr{T}(\epsilon,\gamma,\alpha,R), \tag{2.25}$$

in which the truncation error is extremely complicated algebraically, but satisfies

$$\mathscr{T}(\epsilon,\gamma,\alpha,R) = o(\gamma,\alpha,R), \quad \epsilon\to 0. \tag{2.26}$$

This scaling therefore gives a (perturbed) flux $\mathscr{Q}$ containing PI terms promoted over GI terms and, as per Pukhnachov's equation (2.5), hydrostatic terms demoted from the leading order. The evolution equation implicit in (2.23), (2.25) and (2.26) may be validated against the generalized-scaling analysis of Noakes *et al.* (2006). Write (2.23), (2.25) and (2.26) as

$$\mathscr{H}_t + \mathscr{H}_\theta = g_0\gamma + a_0\alpha + r_0 R + o(\gamma,\alpha,R), \quad \epsilon\to 0, \tag{2.27}$$

in which

$$g_0 = [\mathscr{H}^3\cos\theta]_\theta, \quad a_0 = -[\mathscr{H}^3(\mathscr{H}_\theta + \mathscr{H}_{\theta\theta\theta})]_\theta, \quad r_0 = -[\mathscr{H}^3\mathscr{H}_\theta]_\theta. \tag{2.28}$$

Now consider the two-dimensional (exterior-MPP) form of (3.13) in Noakes *et al.* (2006) which, in the present notation, becomes

$$(1+\epsilon H)(H_t+H_\theta)-\left[\left(H^3+\tfrac{1}{2}\epsilon H^4\right)P^\dagger_\theta\right]_\theta=0, \tag{2.29}$$

in which the two-dimensional *reduced pressure* of Noakes *et al.* (2006, (3.14)) becomes

$$P^\dagger=\gamma(1+\epsilon H)\sin\theta-\alpha(H+H_{\theta\theta})-\epsilon\beta^\dagger H \tag{2.30}$$

where $\beta^\dagger=\epsilon^2a^2\omega\rho/(3\mu)$. Thus, via (2.1) and (2.24), the last term in (2.30) is $-RH$. Eliminating $P^\dagger$ between (2.29) and (2.30) and then using (2.21) to express H in terms of $\mathscr{H}$ and (2.28) to simplify notation, the evolution equation of Noakes *et al.* (2006) becomes

$$\begin{aligned}\mathscr{H}_t+\mathscr{H}_\theta=g_0\gamma+a_0\alpha+r_0R+\tfrac{1}{2}\epsilon(\mathscr{H}_t+\mathscr{H}_\theta)\\ +\epsilon(g_1\gamma+a_1\alpha+r_1R)+O(\epsilon^2\gamma,\epsilon^2\alpha,\epsilon^2R),\end{aligned} \tag{2.31}$$

in which direct calculation yields

$$g_1=-\left[\mathscr{H}^3\left(\mathscr{H}_\theta\sin\theta+\tfrac{3}{2}\cos\theta\right)\right]_\theta \tag{2.32}$$

$$a_1=\left[\mathscr{H}^3\left\{2(1-\mathscr{H})(\mathscr{H}_\theta+\mathscr{H}_{\theta\theta\theta})-3\mathscr{H}_\theta\mathscr{H}_{\theta\theta}\right\}\right]_\theta \tag{2.33}$$

$$r_1=2\left[\mathscr{H}^3(1-\mathscr{H})\mathscr{H}_\theta\right]_\theta, \tag{2.34}$$

so that g_0, a_0, r_0, g_1, a_1 and r_1 are of order $O(1)$ for the thin film under consideration. Hence (2.31) can be solved asymptotically for $\mathscr{H}_t+\mathscr{H}_\theta$ to give

$$\begin{aligned}\mathscr{H}_t+\mathscr{H}_\theta&=g_0\gamma+a_0\alpha+r_0R\\ &\quad+\epsilon\left(\gamma\left[\tfrac{1}{2}g_0+g_1\right]+\alpha\left[\tfrac{1}{2}a_0+a_1\right]+R\left[\tfrac{1}{2}r_0+r_1\right]\right)+O(\epsilon^2\gamma,\epsilon^2\alpha,\epsilon^2R)\\ &=g_0\gamma+a_0\alpha+r_0R+o(\gamma,\alpha,R),\quad \epsilon\to0,\end{aligned} \tag{2.35}$$

which is (2.27). A similar argument is used in (A44)–(A45) in Benilov & O'Brien (2005), in which a zeroth-order approximation for their h_t+h_θ is resubstituted into the first-order terms and then asymptotic equivalence invoked. Thus the evolution equation (2.27) for $\mathscr{H}$ is asymptotically consistent with the benchmark equation of Noakes *et al.* (2006), in which PI terms dominate GI terms and hydrostatic effects are absent at leading order. Ignoring the unspecified asymptotic errors in (2.27) or (2.35), we subsequently consider the evolution equation

$$\mathscr{H}_t+\left\{\mathscr{H}-\gamma\mathscr{H}^3\cos\theta+\alpha\mathscr{H}^3(\mathscr{H}_\theta+\mathscr{H}_{\theta\theta\theta})+R\mathscr{H}^3\mathscr{H}_\theta\right\}_\theta=0. \tag{2.36}$$

Note that if the sign of the inertial term in (2.36) is changed, along with both signs in (2.20), the corresponding interior MPP can be similarly analysed. The automated *Maple* derivation of (2.36) via substitution of (2.21) and (2.24) into (2.14) takes a further 6.23 s, giving a total of approximately 1 min on the modest PC used.

By comparing (2.36) with (2.5), it is now seen that Pukhnachov's equation is therefore asymptotically consistent and mass preserving provided that: its H is identified not with the film height but with the perturbed normalized film height $\mathscr{H}$ of (2.20); the initial film is of uniform thickness, and the original Reynolds number R_0 is scaled with ϵ^3 rather than ϵ^2. Although the evolution equation (2.36) together with the initial condition $\mathscr{H}(\theta,0)=1$ is analysed using two-timescale asymptotics in the next section, a naïve-expansion solution in powers of ϵ of the evolution equation (2.23) prior to the rescaling (2.24) is readily automated in *Maple*. Here we implement explicit exact inversion (rather than *Maple*'s inherent `pdsolve` command) of the differential

	EG	G	O	GW
$f \equiv (\rho\sigma^3/9g\mu^4)^{1/2}$	93.18	0.03048	110.6	4.958

TABLE 1. Fluid-specific factors f to be used in computing the rescaled Reynolds number R for ethylene glycol (EG), glycerine (G), oil (O) and an 85 %–15 % glycerine–water mixture (GW). If $\gamma_0 = 10^x$, $\alpha_0 = 10^y$ and $\epsilon = 10^{-z}$, R in (2.40) is given by $10^{(x-3y-6z)/2} f$. In computations in Hinch & Kelmanson (2003), $x \approx 1.0969$, $y = 1$ and $z \approx 0.9470$ give $R \approx 10^{-3.7925} f$ so that $R_{EG} \approx 0.01502$, $R_G \approx 4.914 \times 10^{-6}$, $R_O \approx 0.01783$ and $R_{GW} \approx 7.994 \times 10^{-4}$. For these x, y and z, $\gamma \approx 0.05319$ and $\alpha \approx 0.004807$, and hence the positioning of $R \ll 1$ in the hierarchy (2.39) is fluid dependent. Moreover, $\alpha\gamma^2 \approx 1.340 \times 10^{-5}$ and so the balance $R = O(\alpha\gamma^2)$ discussed after (2.38) is physically possible. Tabulated values of f were computed using data (in SI units) measured at 100 kPa and 288 K, together with a value of $g = 9.81\ \mathrm{m\,s^{-2}}$.

operators arising at each level of the ϵ hierarchy. For $N = 10$, requiring 12.68 s, the series solution for $\mathscr{H}$ contains, *inter alia*, the fundamental-mode terms

$$-\tfrac{1}{3}\epsilon^2\gamma_0\left\{1 + \tfrac{1}{3}\epsilon^3 R_0 t + \tfrac{1}{18}\epsilon^6 R_0^2 t^2 + \cdots - \tfrac{7}{2}\epsilon^7\alpha_0\gamma_0^2 t + \cdots\right\}\cos(\theta - t) \tag{2.37}$$

and the first-harmonic terms

$$\tfrac{1}{6}\epsilon^4\gamma_0^2\left\{1 + \epsilon^3(2R_0 - 4\alpha_0)t + \epsilon^6\left(\tfrac{14}{9}R_0^2 - \tfrac{20}{3}R_0\alpha_0 + 8\alpha_0^2\right)t^2 + \cdots\right\}\cos 2(\theta - t). \tag{2.38}$$

The secularities in (2.37) suggest exponential growth of the fundamental mode, on the timescale $\epsilon^3 R_0 t$, that opposes the exponential decay on the slower timescale $\epsilon^7\alpha_0\gamma_0^2 t$ discovered by Hinch & Kelmanson (2003) in the case $R_0 = 0$. Hence the balance $R_0 = O(\epsilon^4\alpha_0\gamma_0^2)$, equivalently $R = O(\alpha\gamma^2)$, quantifies the destabilizing centrifugal effect on the fundamental mode, thereby addressing the 'further investigation' proposed by Noakes *et al.* (2006, p. 179). The secularities in (2.38) suggest that first and higher harmonics may also remain undamped when $R_0 = O(\alpha_0)$, equivalently $R = O(\alpha)$, because of the opposite signs of the coefficients in the implied exponential. The naïve expansion for $\mathscr{H}$ suggests no leading-order changes to the $O(\epsilon^4\gamma_0^2)$, equivalently $O(\gamma^2)$, inertia-free drift rate found in Hinch & Kelmanson (2003).

By (2.24), small parameters γ and α satisfy the hierarchy

$$\gamma^2 \ll \alpha \ll \gamma \ll 1 \tag{2.39}$$

when $\gamma_0,\ \alpha_0 \ll O(\epsilon^{-2})$. By (2.15), γ_0 and α_0 link all three of the non-dimensional parameters in (2.1), hence their specification fixes the Reynolds number which, by (2.1), (2.15) and (2.24), has the rescaled form

$$R = \left(\frac{\gamma_0\rho\sigma^3\epsilon^6}{9\alpha_0^3 g\mu^4}\right)^{1/2} = \left(\frac{\gamma\rho\sigma^3\epsilon^{13}}{81\alpha^3 g\mu^4}\right)^{1/2}. \tag{2.40}$$

With the hierarchy (2.39), it is the case that $O(\alpha) \gg O(\alpha\gamma^2)$ and hence, of the balances discussed above, it is $R = O(\alpha\gamma^2)$ that governs the inertial destabilization of surface-tensional decay. Values of R can be computed for a selection of fluids using the information given in table 1, in whose caption an example reveals two noteworthy points: first, the positioning of the small parameter R within the hierarchy (2.39) is preordained by a particular fluid's physical properties, and, second, the $R = O(\alpha\gamma^2)$ balance required to negate surface-tension damping of the fundamental mode is physically realizable in practice. Thus physically motivated, analysis of the inertial destabilization of surface-tension decay is now undertaken.

3. Two-timescale approximation of $\mathscr{H}(\theta, t)$

Hinch & Kelmanson (2003) derive an $(N+1)$-term solution $H_N(\theta, t)$ of (2.5), as a series in γ, using two-timescale asymptotics employing fast and slow timescales $\tau = t$ and $T = \gamma^2 t$, respectively, the latter being discovered through numerical integrations of (2.5) and physically explained via a complex double action of gravity on free-surface harmonic modes. Below, hybrid strained-coordinate/two-timescale asymptotics (Kevorkian & Cole 1996, ch. 4) are used to obtain an approximate solution $\mathscr{H}_N(\theta, t)$ of (2.36) in which the fast timescale is strained in the form $\tau = (1 + \sum_{k\in\mathbb{N}} \omega_k \gamma^k)t$ wherein the ω_k are to be determined. By so straining the fast timescale to accommodate the cumulative effect of gravitational drift, the algebraic simplification can be made of confining slow-timescale activity of the fundamental mode entirely to decay. The slow timescale is again $T = \gamma^2 t$, by which $\omega_{2k-1} = 0$, $k \in \mathbb{N}$, so that $\partial_t = (1 + \sum_{k\in\mathbb{N}} \omega_{2k}\gamma^{2k})\partial_\tau + \gamma^2 \partial_T$.

A solution of (2.36) is sought in the form

$$\mathscr{H}_N(\theta, t) = 1 + \sum_{k=1}^{N} \gamma^k h_k(\theta, \tau, T), \tag{3.1}$$

in which N is specified, the h_k are 2π-periodic in θ, and the uniform initial profile discussed immediately after (2.20) requires $h_k(\theta, 0, 0) = 0$, $k = 1, \ldots, N$. When (3.1) is substituted into (2.36), the partial differential equation for h_k at each order $O(\gamma^k)$ is of the form $\mathscr{L}h_k = r_k(\theta, \tau, T, h_1, \ldots, h_{k-1})$, say, in which the linear differential operator $\mathscr{L}$ is

$$\mathscr{L} \equiv \alpha\partial_\theta^4 + (\alpha + R)\partial_\theta^2 + \partial_\theta + \partial_\tau, \tag{3.2}$$

whose kernel contains the 2π-periodic functions $K_{mn}(\theta, \tau, T)$ given by

$$K_{mn} = (A_{mn}(T)c_{nn} + B_{mn}(T)s_{nn})\,\mathrm{e}^{n^2\{R-(n^2-1)\alpha\}\tau}, \tag{3.3}$$

in which $c_{mn} = \cos(m\theta - n\tau)$, $s_{mn} = \sin(m\theta - n\tau)$, and A_{mn} and B_{mn} are arbitrary functions of T. The form of the slow timescaling has $\partial_T h_k$ first appearing in r_{k+2}. Equation (3.3) explicitly reveals the fundamental difference between the present case and the inertia-free problem considered previously: when $R > 0$, the fundamental mode $(n = 1)$ can decay to a steady state if and only if the surface-tension-induced decay of the slow-timescale functions $A_{11}(T)$ and $B_{11}(T)$ is sufficiently great to counteract the exponential growth $\exp(R\tau)$ on the fast timescale.

At each order $O(\gamma^k)$, $k = 1, \ldots, N$, the initial-value problem $\mathscr{L}h_k = r_k$, $h_k(\theta, 0, 0) = 0$, can be integrated exactly and efficiently. Using the notation $C^p_{mn} = c_{mn}\mathrm{e}^{p\tau}$ and $S^p_{mn} = s_{mn}\mathrm{e}^{p\tau}$, it is straightforward to show that

$$\mathscr{L}^{-1}C^p_{mn} = \frac{\mathscr{A}C^p_{mn} + \mathscr{B}S^p_{mn}}{\mathscr{A}^2 + \mathscr{B}^2} \quad \text{and} \quad \mathscr{L}^{-1}S^p_{mn} = \frac{-\mathscr{B}C^p_{mn} + \mathscr{A}S^p_{mn}}{\mathscr{A}^2 + \mathscr{B}^2}, \tag{3.4}$$

in which $\mathscr{A} = \alpha m^4 - (\alpha + R)m^2 + p$ and $\mathscr{B} = m - n$: the case $\mathscr{A} = \mathscr{B} = 0$ accounts for the fast-timescale elements in K_{mn} in (3.3). Each right-hand side r_k is first partitioned into constituents, defined by different values of p, all of which contain R and some of which also contain α (see § 4). Each such constituent is then swept systematically to find the (m, n) distribution of its c_{mn} and s_{mn} harmonics for $m = 1, \ldots, N$ and $n = -N, \ldots, N$, the negative values of n admitting reflected wave modes moving against the direction of rotation; this effectively defines a matrix of coefficients for the inversions in (3.4). Complementary functions and particular integrals based upon (3.3) and (3.4) can then be constructed and assembled to give h_m. As per the analysis

in §2, the entire procedure has been implemented and fully automated in *Maple*. The bespoke automated integration procedure is both faster than *Maple*'s inherent `pdsolve` command, and it reveals the solution structure in a succinct and physically interpretable form.

The equation at order $O(\gamma)$ is $\mathscr{L}h_1 = -s_{10}$, the only forcing term arising from the steady state, with solution

$$h_1(\theta,\tau,T) = \frac{c_{10}+Rs_{10}}{1+R^2} + A_{11}C_{11}^R + B_{11}S_{11}^R, \tag{3.5}$$

whose components (the last two of which constitute K_{11}) represent a combination of a steady state and a fundamental mode modulated slowly by surface tension and rapidly by inertia. The initial condition for h_1 gives

$$A_{11}(0) = -\frac{1}{1+R^2} \quad \text{and} \quad B_{11}(0) = -\frac{R}{1+R^2}. \tag{3.6}$$

Solution of the $O(\gamma)$ problem requires 0.06s CPU. It is seen from (3.5) that a stable solution requires the exponential fast-timescale growth terms C_{11}^R and S_{11}^R to be dampened by the slow-timescale decay terms A_{11} and B_{11}.

The equation at order $O(\gamma^2)$ is $\mathscr{L}h_2 = r_2$, with

$$\begin{aligned} r_2 = {} & \frac{3}{(1+R^2)^2}(2Rc_{20} - (1-R^2)s_{20}) \\ & + \frac{3}{1+R^2}\{(2RA_{11} + (1-R^2)B_{11})C_{21}^R - ((1-R^2)A_{11} - 2RB_{11})S_{21}^R\} \\ & + 3R\{(A_{11}^2 - B_{11}^2)C_{22}^{2R} + 2A_{11}B_{11}S_{22}^{2R}\}, \end{aligned} \tag{3.7}$$

in which the contributions to the forcing term are from, in the order presented: the steady state, interaction between the steady state and the fundamental mode, and self-excitation of the fundamental mode. The solution of $\mathscr{L}h_2 = r_2$ is

$$\begin{aligned} h_2(\theta,\tau,T) = {} & \frac{3(\lambda_{20}c_{20} - 2\mu_{20}s_{20})}{2(1+R^2)^2(1+4(R-3\alpha)^2)} \\ & + \frac{3\big((\lambda_{21}A_{11} + \mu_{21}B_{11})C_{21}^R - (\mu_{21}A_{11} - \lambda_{21}B_{11})S_{21}^R\big)}{(1+R^2)(1+9(R-4\alpha)^2)} \\ & + \frac{3}{2(6\alpha - R)}\{(A_{11}^2 - B_{11}^2)C_{22}^{2R} + 2A_{11}B_{11}S_{22}^{2R}\} \\ & + A_{22}C_{22}^{4(R-3\alpha)} + B_{22}S_{22}^{4(R-3\alpha)}, \end{aligned} \tag{3.8}$$

in which $\lambda_{20} = 1 + 12R\alpha - 5R^2$, $\mu_{20} = 3\alpha - 2R - 3R^2\alpha + R^3$, $\lambda_{21} = 1 + 24R\alpha - 7R^2$ and $\mu_{21} = 12\alpha - 5R - 12R^2\alpha + 3R^3$. The first three components on the right-hand side of h_2 in (3.8) are particular integrals for the three components of r_2 in (3.7), and the fourth is K_{22}, in the kernel of $\mathscr{L}$. The initial condition for h_2 gives

$$A_{22}(0) = \frac{3(R-3\alpha)(1-6(R-3\alpha)(R-4\alpha))}{(R-6\alpha)(1+4(R-3\alpha)^2)(1+9(R-4\alpha)^2)}, \tag{3.9}$$

$$B_{22}(0) = \frac{3(R-3\alpha)(5R-18\alpha)}{(R-6\alpha)(1+4(R-3\alpha)^2)(1+9(R-4\alpha)^2)}. \tag{3.10}$$

Solution of the $O(\gamma^2)$ problem requires 1.17 s CPU. Note that slow-timescale functions A_{11} and B_{11} introduced at order $O(\gamma)$ are still not determined, and hence neither is h_1. The double action of gravity defers this to the order $O(\gamma^3)$ problem, in which

suppression of secularity, in conjunction with (3.6), determines A_{11} and B_{11}. By the same process, h_2 cannot be fully determined until suppression of secularities in the order $O(\gamma^4)$ problem, in conjunction with (3.9) and (3.10), determines A_{22} and B_{22}. Note also that the simplification invoked by Hinch & Kelmanson (2003) – effectively, the discarding of all K_{nn} terms with $n > 1$ – cannot be repeated because such terms do not now become exponentially small when $\tau = O(1)$ due to the opposition of surface tension by inertia. This augurs a significant increase in algebraic complexity of the problems at subsequent orders of γ.

At order $O(\gamma^3)$ the equation $\mathscr{L}h_3 = r_3$ has, after combining (i.e. reducing) r_3 into a linear combination of harmonics, 1526 terms comprising: 46 in the secular factor of $\mathrm{e}^{R\tau}$ (from the fundamental mode K_{11}); 200 in the non-secular factor of $\mathrm{e}^{R\tau}$ (from the interaction between the fundamental mode and the steady state); 437 in the non-secular factor of $\mathrm{e}^{2R\tau}$ (from self-excitation of the fundamental mode); 240 in the non-secular factor of $\mathrm{e}^{3R\tau}$ (from repeated self-excitation of the fundamental mode); 248 in the non-secular factor of $\mathrm{e}^{(4R-12\alpha)\tau}$ (from the first harmonic K_{22}); 288 in the non-secular factor of $\mathrm{e}^{(5R-12\alpha)\tau}$ (from the interaction between the fundamental mode and the first harmonic) and 67 pure-trigonometric (from the steady state).

The solution h_1 of the order $O(\gamma)$ problem is first completed by determining A_{11} and B_{11} from the 46 terms in the secular factor of $\mathrm{e}^{R\tau}$, which yield two 23-term coupled ordinary differential equations of the form

$$\partial_T A_{11} = \delta_3 A_{11} - \eta_3 B_{11} \quad \text{and} \quad \partial_T B_{11} = \eta_3 A_{11} + \delta_3 B_{11}, \tag{3.11}$$

in which δ_3 and η_3 are known functions of R, α and ω_2. The value of ω_2 is not yet determined uniquely; when expressed in the form

$$\omega_2 = \frac{3(15R^2 - 36R\alpha - 72\alpha^2 - 5)}{2(1+R^2)(1+9(R-4\alpha)^2)} + \epsilon_0, \tag{3.12}$$

in which ϵ_0 is an arbitrary constant, the drift factor η_3 vanishes when $\epsilon_0 = 0$. With ω_2 thus defined, the decay factor δ_3 is given by

$$\delta_3 = -\frac{9(4R^3 - 15R^2\alpha - 4R + 9\alpha)}{(1+R^2)(1+9(R-4\alpha)^2)} - R\epsilon_0. \tag{3.13}$$

The value $\epsilon_0 = 0$ is chosen to confine drift of the fundamental mode (but not of the higher harmonics) to the strained timescale τ: this is consistent with having used the unstrained fast timescale $\tau = t$, which at this order gives the first term on the right-hand side of (3.12) uniquely as ω_2. The small-R expansion of (3.12) is then

$$\omega_2 \approx -\frac{3(5+72\alpha^2)}{2(1+144\alpha^2)} - \frac{54\alpha(11+288\alpha^2)}{(1+144\alpha^2)^2}R + O(R^2),$$

in which the first term on the right-hand side is the value of ω_2 found by Hinch & Kelmanson (2003) in the case $R = 0$, and the second term shows that the counter-rotational drift is increased in the presence of inertia. When $\epsilon_0 = 0$ the small-R expansion of (3.13) is

$$\delta_3 \approx -\frac{81\alpha}{1+144\alpha^2} + \frac{36(1-18\alpha^2)}{(1+144\alpha^2)^2}R + O(R^2),$$

in which the first term on the right-hand side is the fundamental-mode slow-timescale decay rate found by Hinch & Kelmanson (2003) in the case $R = 0$, and the second term, positive because $\alpha \ll 1$, quantifies the inertial (centrifugal) destabilization of such decay.

Using the initial conditions (3.6), the slow-timescale modulation functions for the fundamental mode are now determined as

$$A_{11}(T) = -\frac{\exp(\delta_3 T)}{1+R^2} \quad \text{and} \quad B_{11}(T) = -\frac{R\exp(\delta_3 T)}{1+R^2}. \tag{3.14}$$

With h_1 fully determined and ω_2 known, the automated procedure described above is again used to determine particular integrals for the remaining 1480 non-secular terms in r_3. Finally, h_3 is constructed from these particular integrals augmented by K_{33} and K_{31}, the latter of which is also in the kernel of $\mathscr{L}$ and whose presence is required because the initial condition $h_3(\theta, 0, 0) = 0$ includes not only c_{30} and s_{30} but also c_{10} and s_{10}. By this addition, unique values are assigned to $A_{31}(0)$, $B_{31}(0)$, $A_{33}(0)$ and $B_{33}(0)$. Algebraic details of h_3 are cumbersome and therefore omitted. Solution of the $O(\gamma^3)$ problem requires 23.90 s CPU.

At this stage, A_{22} and B_{22} in h_2 are still unknown, and h_3 contains the six unknown functions A_{22}, B_{22}, A_{31}, B_{31}, A_{33} and B_{33}. The evolution equations for A_{22} and B_{22} are determined from only a partial analysis of the order $O(\gamma^4)$ equation $\mathscr{L}h_4 = r_4$; specifically, by annihilating in r_4 the coefficients of the secular terms $C_{22}^{4(R-3\alpha)}$ and $S_{22}^{4(R-3\alpha)}$. It is computationally expensive, increasingly difficult to automate and digressional to the goal of this paper, to complete both the order $O(\gamma^4)$ and order $O(\gamma^5)$ problems to determine not only the evolution equations for A_{31}, B_{31}, A_{33} and B_{33}, but also the next coefficient ω_4 in the strained timescale τ. It is feasible to do this systematically in the case $R = 0$, and this has been done, using a *pseudo-three-timescale* technique in Kelmanson (2009), which extends by orders of magnitude the duration of uniform validity of the asymptotic expansions in Hinch & Kelmanson (2003).

The right-hand side of the equation $\mathscr{L}h_4 = r_4$ contains 34 terms in each of the coefficients of the secular $C_{22}^{4(R-3\alpha)}$ and $S_{22}^{4(R-3\alpha)}$. These yield coupled ordinary differential equations of the form

$$\partial_T A_{22} = \delta_4 A_{22} - \eta_4 B_{22} \quad \text{and} \quad \partial_T B_{22} = \eta_4 A_{22} + \delta_4 B_{22}, \tag{3.15}$$

in which δ_4 and η_4 are known functions of R and α. By contrast with (3.11), there is no free parameter in (3.15) and so η_4 cannot be annihilated. Hence the first harmonic contains a component of drift on the slow timescale T over and above that included in the strained timescale τ, and so it (and, presumably, higher harmonics) disperses relative to the fundamental mode. Evolution equations (3.15) have solution

$$A_{22}(T) = (A_{22}(0)\cos\eta_4 T + B_{22}(0)\sin\eta_4 T)\exp(\delta_4 T) \tag{3.16}$$

$$B_{22}(T) = (B_{22}(0)\cos\eta_4 T - A_{22}(0)\sin\eta_4 T)\exp(\delta_4 T) \tag{3.17}$$

in which (3.9) and (3.10) give $A_{22}(0)$ and $B_{22}(0)$. The explicit forms of δ_4 and η_4 are cumbersome: they are approximated by

$$\delta_4 \approx -\frac{54\alpha(23-360\alpha^2)}{1+3600\alpha^2} + 114R + O(R\alpha^2, R^2),$$

$$\eta_4 \approx -\frac{1944\alpha(37+144\alpha^2)}{(1+144\alpha^2)(1+3600\alpha^2)} + 13\,284R\alpha + O(R\alpha^3, R^2).$$

Completing the order $O(\gamma^2)$ problem (i.e. fully determining h_2) by partial solution of the $O(\gamma^4)$ problem requires 3.34 s CPU. Finally, the three-term two-timescale approximation of the perturbed film height is constructed using (3.1) and, to accelerate the convergence of the sum of these three terms, the [1/1]-Padé approximant $\widetilde{\mathscr{H}}_2$ of

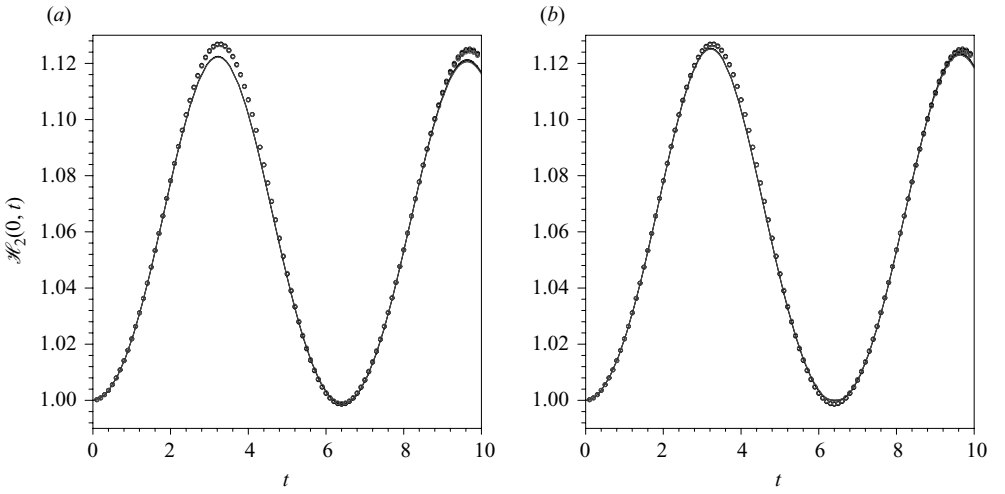

FIGURE 1. (*a*) Continuous lines are the time evolution of $\mathscr{H}_2(0,t)$ and (*b*) its [1/1]-Padé approximant $\widetilde{\mathscr{H}}_2(0,t)$, as defined in (3.18), for $0 \leqslant t \leqslant 10$. The small circles are numerical data extrapolated from fourth-order finite-difference results computed using 50 and 100 equally spaced nodes around the cylinder. Parameters $\gamma \approx 0.05319$ and $\alpha \approx 0.004807$ (as used in table 1 and Hinch & Kelmanson 2003) are used throughout, and there are three curves, visually indistinguishable at this scale in this time interval, corresponding to $R = 0,\ 5.0 \times 10^{-4}$ and 1.0×10^{-3}. The [1/1]-Padé approximant improves the asymptotic solution near the maxima but reduces accuracy near the minima, where the approximant is ill-conditioned because $\gamma, |h_1|, |h_2| \ll 1$.

$\mathscr{H}_2$ is also considered, i.e.

$$\mathscr{H}_2 = 1 + \gamma h_1 + \gamma^2 h_2 \quad \text{and} \quad \widetilde{\mathscr{H}}_2 = \frac{h_1 + \gamma\left(h_1^2 - h_2\right)}{h_1 - \gamma h_2}. \tag{3.18}$$

Figures 1 and 2 show comparisons between $\mathscr{H}_2$ and $\widetilde{\mathscr{H}}_2$ for specific parameter values; they also compare both solutions with extrapolated fourth-order finite-difference results. Figure 3 shows the increasing drift between $\mathscr{H}_2$ and numerical data at large times.

An alternative two-timescale approach to the above is to subtract out both the steady-state component $\mathscr{H}_s(\theta)$ of the solution (computed in § 5 to a high order of γ) and gravitationally induced drift to leave evolution equations governing only decay or growth on the slow timescale. Since (3.12) gives

$$\omega_2 = -\tfrac{15}{2}\gamma^2 + O(\alpha R, \gamma^4),$$

leading-order drift is removed via the coordinate transformation

$$\psi = \theta - (1 - (15/2)\gamma^2)t,$$

using which $\mathscr{H}(\theta, t)$ is expanded as

$$\mathscr{H}(\theta, t) = \mathscr{H}_s(\theta) + \sum_n \gamma^n h_n(\theta, \psi, T),$$

as in Hinch *et al.* (2004, § 3). With $\alpha = \alpha_2\gamma^2$, $R = R_2\gamma^2$ and the slow timescale $T = \gamma^2 t$, this leads to $h_1(\theta, \psi, T) = f(\psi, T)$ and the initial condition $f(\psi, 0) = -\cos\psi$, where $f(\psi, T)$, the order $O(\gamma)$ component of $\mathscr{H}$, satisfies the linear evolution equation

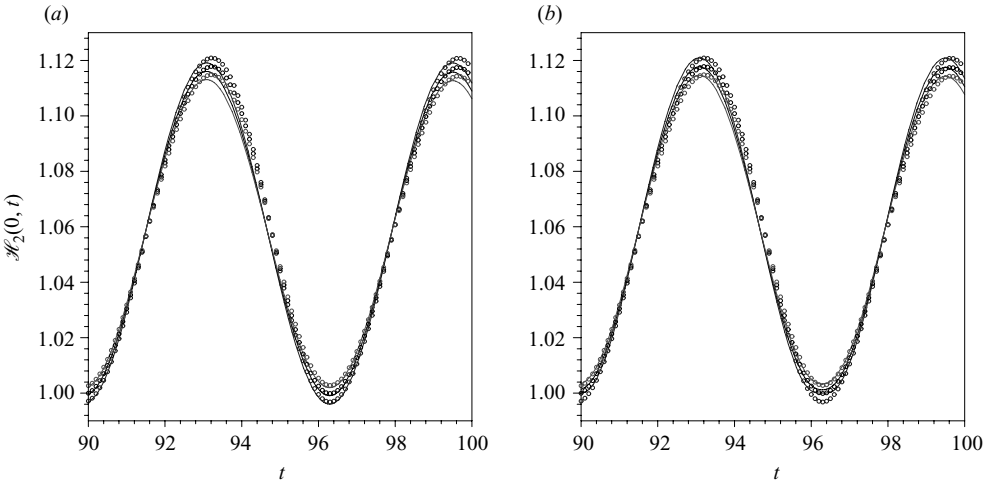

FIGURE 2. Caption as per figure 1, but for $90 \leqslant t \leqslant 100$. By this time, the three curves corresponding to $R = 0$, 5.0×10^{-4} and 1.0×10^{-3} have separated because of the cumulative larger-time inertial destabilization of surface-tension-induced decay: the outermost curve, with the smallest minima and the largest maxima, corresponds to the largest value of R. Because ω_4 is not determined in the strained timescale τ, there is little point in detailed comparisons between theoretical and numerical results beyond this time, and figure 3 shows an order $O(1)$ drift between theory and computation when $t = O(10^3)$.

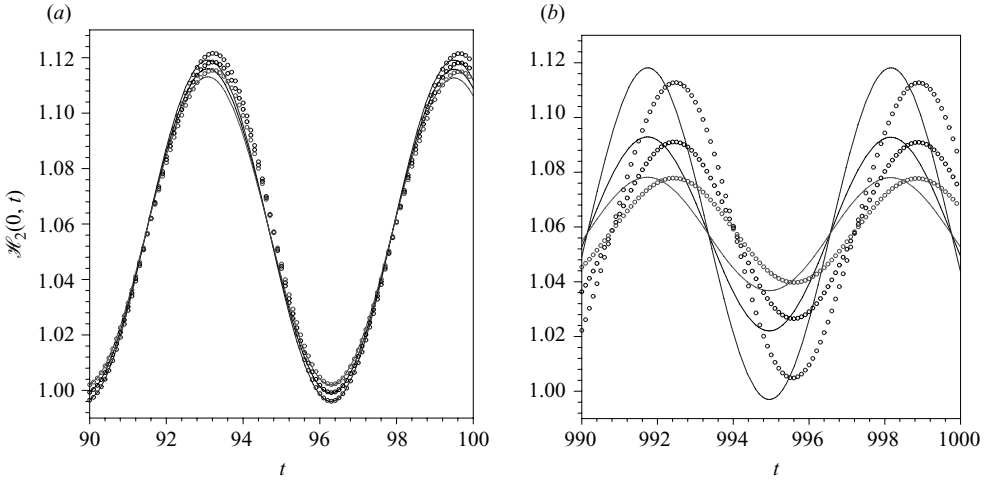

FIGURE 3. Comparison between $\mathscr{H}_2(0,t)$ (lines) and numerical data (circles) for (*a*) $t = O(10^2)$ and (*b*) $t = O(10^3)$, for the parameters in the caption of figure 1 and $R = 0$ (most rapidly decaying), $R = 5.0 \times 10^{-4}$ and $R = 1.0 \times 10^{-3}$ (least rapidly decaying). At the later time, the inertial destabilization of surface-tension decay is clearly evidenced (the vertical scales on both plots are identical) and the value of $R = 1.0 \times 10^{-3}$ appears to be close to the critical value that exactly balances the decaying action of surface tension. An order $O(1)$ drift is visible at the later time between the theoretical and numerical results because of the absence of the ω_4 term in the strained timescale τ.

(a secularity condition at order $O(\gamma^3)$)

$$\left(\partial_T + \alpha_2\partial_\psi^4 + (\alpha_2 + R_2)\partial_\psi^2\right) f = 0,$$

in which the operator should be compared with that in (3.2). With $\alpha = \alpha_3\gamma^3$, $R = R_3\gamma^3$ and the slow timescale $T = \gamma^3 t$ associated with shock formation, $f(\psi, T)$ satisfies the nonlinear evolution equation (a secularity condition at order $O(\gamma^4)$)

$$\left(\partial_T - 30f\partial_\psi + \alpha_3\partial_\psi^4 + (\alpha_3 + R_3)\partial_\psi^2\right) f = 0,$$

which can be solved by suitably amending the analysis in Hinch *et al.* (2004, §§4 and 5). A related (component) evolution equation in Noakes *et al.* (2006, (3.55)) includes a quintic term that translates to $-\partial_{\psi_0}((3/2)\gamma^2 H_0^5)$ in the present scaling, in which H_0 is the leading-order component of H and $\psi_0 = \theta - t = \psi + (15/2)\gamma^2 t$. By (2.4) in Hinch *et al.* (2004), the argument of $-\partial_{\psi_0}$ is precisely the first perturbation in the action variable of the Hamiltonian for H derived in the limit $\alpha, R \to 0$ which, by (2.6) and (2.8) in Hinch *et al.* (2004), gives rise to a leading-order gravitational drift rate of $-(15/2)\gamma^2$ relative to the uniformly changing coordinate ψ_0. That is, ψ_0 and ψ respectively admit and remove drift in their corresponding evolution equations, and the quintic term in the former has been implicitly accommodated in the latter simply by straining the fast timescale; both approaches are therefore asymptotically consistent.

4. Inertial effects

Inspection of (3.8) reveals that $\mathscr{H}_2$ contains terms whose denominator may vanish when R is certain integer multiple of α; by (2.15) and (2.24), this is equivalent to the Weber number W_0 assuming these integer values. This unexpected potential singularity can be addressed by a combination of mathematical and physical arguments.

The fundamental mode K_{11} in h_1 at order $O(\gamma)$ gives rise to two related types of contributions of the order $O(\gamma^k)$ problem for all $k > 1$. First, via the nonlinear occurrence of h_1 in r_k, K_{11} produces terms of the form $\mathscr{P}_C^{(k)} C_{kk}^{kR}$ and $\mathscr{P}_S^{(k)} S_{kk}^{kR}$, in which $\mathscr{P}_C^{(k)}$ and $\mathscr{P}_S^{(k)}$ are homogeneous polynomials of degree k in A_{11} and B_{11}. For example, (3.8) reveals that C_{22}^{2R} and S_{22}^{2R} have potentially vanishing denominators in h_2, as do C_{33}^{3R} and S_{33}^{3R} in h_3. Equation (3.4) reveals that C_{kk}^{kR} and S_{kk}^{kR} are in the kernel of $\mathscr{L}$ when $\alpha k^4 - (\alpha + R)k^2 + kR = 0$, i.e. $R = k(k+1)\alpha$, $k = 2, \ldots, N$. Hence $R = 6\alpha,\ 12\alpha,\ 20\alpha, \ldots$ are critical values that potentially give singular (N.B. not secular) solutions, explaining the appearance of

$$\frac{C_{22}^{2R}}{R - 6\alpha} \text{ and } \frac{S_{22}^{2R}}{R - 6\alpha} \text{ in } h_2, \quad \frac{C_{33}^{3R}}{R - 12\alpha} \text{ and } \frac{S_{33}^{3R}}{R - 12\alpha} \text{ in } h_3, \text{ etc.}$$

Second, K_{11} from h_1 combines with K_{22} from h_2 to produce terms of the form $C_{11}^{5R-12\alpha}$, $S_{11}^{5R-12\alpha}$, $C_{33}^{5R-12\alpha}$, $S_{33}^{5R-12\alpha}$ in h_3. In this case (3.4) reveals that C_{kk}^{p} and S_{kk}^{p} are in the kernel of $\mathscr{L}$ when $\alpha k^4 - (\alpha + R)k^2 + p = 0$ and p is the sum of the exponential indices $n_1^2(R - (n_1^2 - 1)\alpha)$ and $n_2^2(R - (n_2^2 - 1)\alpha)$ for two distinct integers n_1 and n_2 with $1 \leqslant k \leqslant n_1 + n_2$. The values $n_1 = 1$ (from K_{11}) and $n_2 = 2$ (from K_{22}) give $p = 5R - 12\alpha$, from which (3.4) gives the critical values

$$R = \frac{(k-2)(k+2)(k^2+3)}{k^2 - 5}\alpha, \tag{4.1}$$

i.e. $R = 3\alpha,\ 15\alpha$ for $k = 1,\ 3$. This explains the appearance of

$$\frac{C_{11}^{5R-12\alpha}}{R - 3\alpha}, \quad \frac{S_{11}^{5R-12\alpha}}{R - 3\alpha}, \quad \frac{C_{33}^{5R-12\alpha}}{R - 15\alpha} \text{ and } \frac{S_{33}^{5R-12\alpha}}{R - 15\alpha} \text{ in } h_3, \text{ etc.} \tag{4.2}$$

Centrifugal destabilization of decay and the prospect of potential singularity are not the only new features introduced by inertia. Counter-intuitively, it transpires that the two-timescale solution obtained when $R=0$ is not algebraically equivalent to that obtained by letting $R\to 0$ in § 3. However, the difference between the two is relatively minute numerically, as illustrated in figure 4. This difference is an artefact of the two-timescale method used, and is now explained. Define $\mathscr{L}_{\mathbf{0}}$ and h_{k_0} by setting $R=0$ in $\mathscr{L}$ and h_k, respectively, and let $\overline{h}_k$ be the counterpart of h_{k_0} obtained from a two-timescale analysis in which R is *a priori* fixed at zero. Let $\overline{\mathscr{H}}_2$ be the corresponding counterpart of the $\mathscr{H}_{2_0}$ obtained by setting $R=0$ in (3.18). Then

$$\mathscr{L}_{\mathbf{0}}c_{11}=0 \quad \text{and} \quad \mathscr{L}_{\mathbf{0}}s_{11}=0 \tag{4.3}$$

and the fundamental-mode terms in h_1 satisfy

$$\mathscr{L}C_{11}^{R}=0 \quad \text{and} \quad \mathscr{L}S_{11}^{R}=0,$$

of which the limit as $R\to 0$ is compatible with (4.3); thus $h_{1_0}=\overline{h}_1$. Ignoring for the moment the K_{22} term in (3.8), it is also apparently the case that $h_{2_0}=\overline{h}_2$. However, h_3 contains a contribution

$$-\frac{3}{4}\left(A_{11}^2+B_{11}^2\right)\left(A_{11}C_{11}^{3R}+B_{11}S_{11}^{3R}\right)$$

that corresponds to repeated self-excitation of the fundamental mode, and in which

$$\mathscr{L}C_{11}^{3R}=O(R) \quad \text{and} \quad \mathscr{L}S_{11}^{3R}=O(R). \tag{4.4}$$

Although (4.4) is compatible with (4.3) as $R\to 0$, neither C_{11}^{3R} nor S_{11}^{3R} are in the kernel of $\mathscr{L}$ whereas C_{11}^{R} and S_{11}^{R} are, as c_{11} and s_{11} are in the kernel of $\mathscr{L}_{\mathbf{0}}$. Thus although $C_{11}^{3R}\to c_{11}$ and $C_{11}^{R}\to c_{11}$ as $R\to 0$, only the second of these contributes to the secularity condition for the evolution equation for A_{11} whereas the first contributes to the initial condition for A_{31}. A parallel comment applies when replacing 'C' by 'S' and 'A' by 'B'. Specifically, those terms ϕ_k in r_k $(k\geqslant 3)$ for which $\mathscr{L}\phi_k=O(R^m)$ $(m>0)$ switch singularly from the integrable components into the secularity conditions as $R\to 0$, so that $h_{k_0}\neq\overline{h}_k$ for $k\geqslant 2$. Equivalently, such terms switch singularly from fast-timescale integrations to slow-timescale evolution equations as $R\to 0$. For example, the value of $A_{31}(0)$ in this case differs by $-(3/4)C_{11}^{R}$ from the value of $A_{31}(0)$ when $R=0$ and, of the order $O(\gamma^4)$ problem, the A_{22} and B_{22} determined in (3.16) and (3.17) differ considerably from their counterparts when $R=0$; in the latter case, Kelmanson (2009) shows that A_{22} and B_{22} contain terms of the form $\exp(\exp(-\lambda T))$ for some $\lambda>0$.

Figure 4 demonstrates the small numerical discrepancy between $\mathscr{H}_{2_0}$ and $\overline{\mathscr{H}}_2$ due to the difference between h_{2_0} and $\overline{h}_2$. The relative error between $\mathscr{H}_{2_0}$ and $\overline{\mathscr{H}}_2$ for these particular parameters never exceeds 4.0×10^{-4} %, and it vanishes as the exponential factors – i.e. precisely those terms obtained from the secularity conditions affected by the above-mentioned switching – decay to zero at large times. The discrepancy arises because $\mathscr{H}_{2_0}$ and $\overline{\mathscr{H}}_2$ are generalized asymptotic expansions that do not satisfy a uniqueness condition (Murdock 1991, p. 230). Finally, the $\overline{\mathscr{H}}_2(\theta,\tau,T)$ calculated here agrees exactly with the $\overline{\mathscr{H}}_2(\theta,t,T)$ obtained by Hinch & Kelmanson (2003) from more complicated evolution equations incorporating the treatment of drift on the slow timescale.

The above discussion of potential singularities can now be resumed in the physical context of inertial destabilization of surface-tension-induced decay. The products $A_{11}C_{11}^{R}$ and $B_{11}S_{11}^{R}$ in h_1 reveal that the fundamental mode will not decay when there

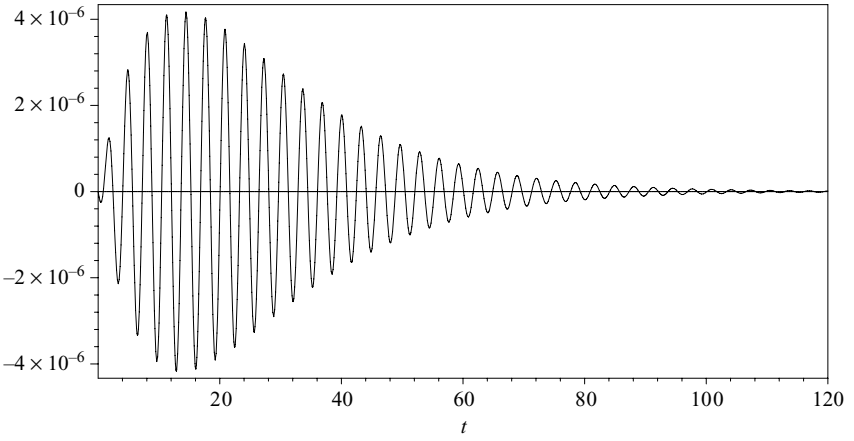

FIGURE 4. Time evolution of the small numerical discrepancy $\mathscr{H}_{2_0} - \overline{\mathscr{H}}_2$ at the station $\theta = 0$ for the parameters $\gamma \approx 0.05319$ and $\alpha \approx 0.004807$ used in Hinch & Kelmanson (2003) and in figures 1–3. The discrepancy tends to zero as $K_{22} \to 0$.

is a balance $\delta_3 T + R\tau = 0$, equivalently

$$\delta_3 \gamma^2 + (1 + \omega_2 \gamma^2) R = 0; \tag{4.5}$$

this same balance arises in h_2 from the second and third terms on the right-hand side of (3.8). Using (3.12) and (3.13), balance (4.5) yields a quintic equation in the critical Reynolds number $R = R_0(\gamma, \alpha)$ with numerical solution $R_0 \approx 1.0164 \times 10^{-3}$ when the parameters given in the caption of table 1 are used. The linearization of (4.5) gives the approximation

$$R_0 \approx \frac{162\alpha\gamma^2}{2 + 288\alpha^2 + 57\gamma^2 - 216\alpha^2\gamma^2}, \tag{4.6}$$

which gives $R_0 \approx 1.0161 \times 10^{-3}$, so that (4.6) has a relative error of only 3.14×10^{-2} %. The leading-order term in the series approximation

$$\widetilde{R}_0 \approx \frac{81\alpha\gamma^2}{1 + 144\alpha^2} + \frac{243(72\alpha^2 - 19)\alpha\gamma^4}{2(1 + 144\alpha^2)^2} \tag{4.7}$$

of the linearization (4.6) comes as no surprise; the merit of (4.7) is that it confirms the expectation that the timescale $\gamma^4 t$ is the next to be used in a three-timescale asymptotic procedure; this information is used in Kelmanson (2009) to pursue a pseudo-three-timescale approximation that increases the duration of uniform validity of the approximate solutions of Hinch & Kelmanson (2003). From the higher harmonics at order $O(\gamma^k)$, $k > 1$, the balance equation is similarly

$$\delta_k \gamma^2 + k^2(1 + \omega_2 \gamma^2)(R - (k^2 - 1)\alpha) = 0$$

which, because $\delta_k = O(\alpha)$ for all $k > 1$, has the solution $R = O(\alpha)$. Thus the potential singularity discussed above can never occur in practice because exponentially growing solutions already occur at the much lower threshold $R = O(\alpha\gamma^2)$ in (4.7). Hence $\mathscr{H}_2$ evaluated with physically realistic parameters is always uniformly valid until $\tau = O(\gamma^{-2})$, equivalently $t = O(\gamma^{-2})$.

With reference to the physical plausibility of the present theory alluded to in the caption of table 1, it is indeed possible to achieve the critical Reynolds number (4.6) in practice. For example, a thin film of glycerine on a roller of diameter 1.01 cm

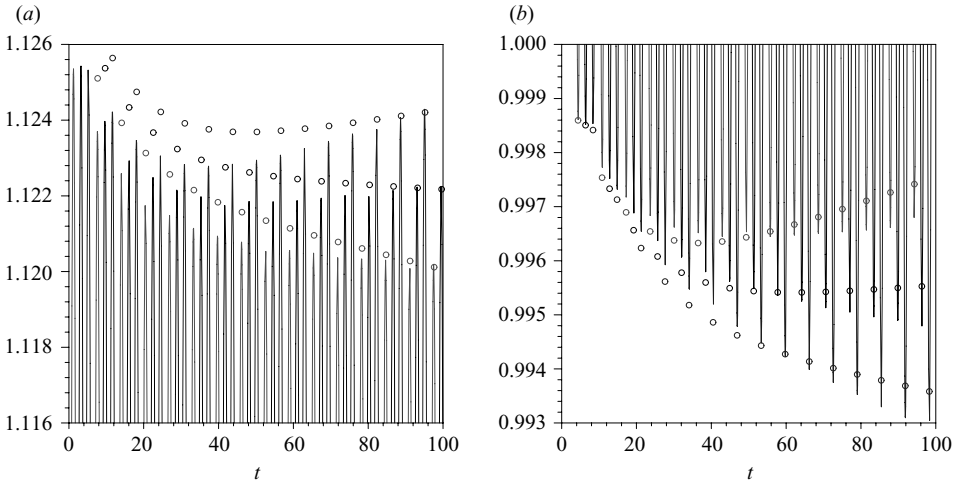

FIGURE 5. Comparison for $0 \leqslant t \leqslant 100$ of $\mathscr{H}_2(0, t)$ (continuous lines) and the (a) maxima and (b) minima of the numerical data (small circles, computed by quadratic Lagrange interpolation) for $\gamma \approx 0.05319$ and $\alpha \approx 0.004807$ and $R = 9.0 \times 10^{-4}$, 1.2×10^{-3} and 1.5×10^{-3}; the largest value of R corresponds to the highest maxima and the lowest minima. In each group of three data, the left-most maxima and minima are at their true abscissae and the others have been displaced to the right by $\Delta t = 2.0$ and $\Delta t = 4.0$ for clarity. The vertical scales are 14 (a) and 20 (b) times larger than those in figures 1–3. The small discrepancy ($\leqslant 0.75\,\%$ of the amplitude in the two figures) between asymptotics and numerics is due to the absence in $\mathscr{H}_2$ of terms $\gamma^n h_n$ for $n \geqslant 3$.

at 100 kPa and 288 K, with the parameters $\gamma_0 = 10$, $\alpha_0 = 2$ and $\epsilon = 0.0872$ (giving $\gamma = 0.02535$ and $\alpha = 4.42 \times 10^{-4}$), reaches the critical value $R \approx 2.259 \times 10^{-5}$ at a rotation rate of $\omega = 42.56$ r.p.m. Moreover, many polymers and molten plastics, with approximately the same density as water and half its surface tension, can be diluted to give a wide range of dynamic viscosities (Brandrup *et al.* 2003), yielding a vast range of industrially relevant parameters accommodated by the present theory. Further discussion of physically realizable parameters may be found in Hinch *et al.* (2004, § 7), which concludes that the asymptotic predictions of several features of this exterior MPP are observable in practice.

For the remainder of this section, however, the parameters used in Hinch & Kelmanson (2003) and figures 1–4 will continue to be used, together with $O(10^{-4}) < R < O(10^{-3})$, in order to analyse harmonic decay discernible over the uniformly valid timescale of order $O(\gamma^{-2})$. The critical value R_0 predicted by (4.6) cannot be expected to agree exactly with that obtained from numerical integrations of (2.5) because it is based upon a balance (4.5) of only the order $O(\gamma)$ fundamental-mode contribution, h_1, to $\mathscr{H}_2$; the neglected contributions from h_k for $k > 1$ will slightly change the value of R_0. Moreover, the absence of $\gamma^3 h_3$ and higher-order terms in $\mathscr{H}_2$ will preclude excellent agreement between $\mathscr{H}_2$ and the numerically obtained $\mathscr{H}$. These effects are illustrated in figure 5, which compares the two-timescale solution (3.18) with numerical integrations of (2.5) for parameters $\gamma \approx 0.05319$ and $\alpha \approx 0.004807$ and $R = 9.0 \times 10^{-4}$, 1.2×10^{-3} and 1.5×10^{-3}, the second of which is close to the critical value of R_0 in the numerical data; in relative terms, the numerical and theoretical amplitudes differ by only 0.75 %. Figure 6 shows a comparison between the two-timescale and numerical solutions for the (numerical) critical value $R = 1.2 \times 10^{-3}$,

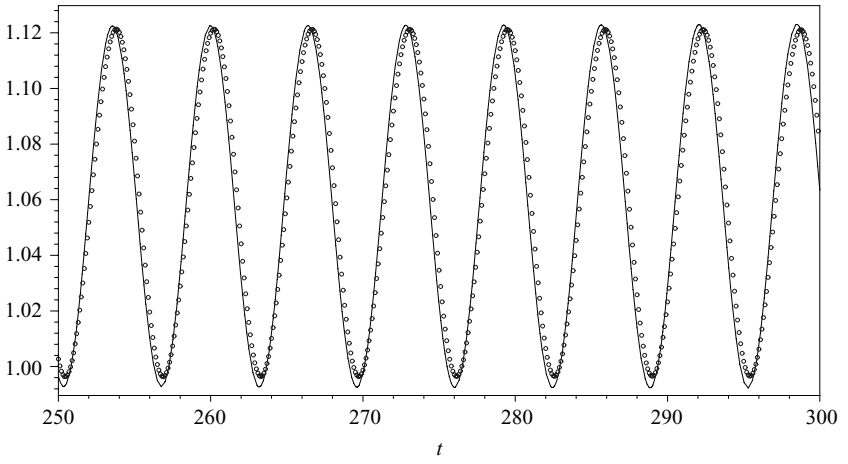

FIGURE 6. Large-time comparison of $\mathscr{H}_2(0,t)$ (continuous line) and Richardson-extrapolated numerical data (circles) for $R=1.2\times10^{-3}$, close to the critical value of R dictated by the numerics. No perceptible changes in maxima or minima occur on this scale.

in which, on the presented scale, there is no perceptible change in amplitude of oscillation over the time interval $250\leqslant t\leqslant 300$.

5. Steady-state solution

The steady exterior MPP originally considered in Moffatt (1977) and Pukhnachev (1977) has been revisited by, e.g. Hansen & Kelmanson (1994), Kelmanson (1995), Wilson, Hunt & Duffy (2002), Hinch & Kelmanson (2003), Evans, Schwarz & Roy (2004), Hinch *et al.* (2004), Pukhnachov (2005*a*,*b*) and Karabut (2007), the last two of which place particular emphasis on the existence and uniqueness of asymptotic solutions with $R=0$ in small- and large-α limits. Because of the equivalent scalings and directly comparable asymptotics in Pukhnachev (1977), Pukhnachov (2005*a*,*b*) and Karabut (2007), inertial augmentation of these particular studies is now considered and a number of comparisons are made.

With $\partial_t\equiv0$, one integration of (2.36) with respect to θ yields the third-order ordinary differential equation

$$\mathscr{H}-\gamma\mathscr{H}^3\cos\theta+\alpha\mathscr{H}^3(\mathscr{H}_\theta+\mathscr{H}_{\theta\theta\theta})+R\mathscr{H}^3\mathscr{H}_\theta=\mathscr{Q}, \tag{5.1}$$

in which $\mathscr{Q}$ is defined immediately after (2.21). A solution of (5.1) is sought in the form

$$\mathscr{H}^*_N(\theta,t)=1+\sum_{k=1}^{N}\gamma^k h_k^*(\theta)\quad\text{and}\quad \mathscr{Q}_N=1+\sum_{k=1}^{N}\gamma^k q_k, \tag{5.2}$$

in which N is specified and the h_k^* are 2π-periodic in θ. When (5.2) is substituted into (5.1), the ordinary differential equation for h_k^* at each order $O(\gamma^k)$ is of the form $\mathscr{L}_*h_k^*=r_k(\theta,h_1^*,\ldots,h_{k-1}^*)$, say, in which the linear differential operator $\mathscr{L}_*$ is

$$\mathscr{L}_*\equiv\alpha\partial_\theta^3+(\alpha+R)\partial_\theta+\mathscr{I},$$

where $\mathscr{I}$ is the identity operator and the invertibility of $\mathscr{L}_*$ as $R\to0$ is addressed formally in Pukhnachov (2005*b*). At each order $O(\gamma^k)$, $k=1,\ldots,N$, the

boundary-value problem $\mathscr{L}_* h_k^* = r_k$, $h_k^*(\theta) = h_k^*(\theta + 2\pi)$, is integrated exactly and efficiently using a similar approach to that outlined in § 3. If now $c_m = \cos m\theta$ and $s_m = \sin m\theta$, it is straightforward to show that

$$\mathscr{L}_*^{-1} c_m = \frac{c_m + \mathscr{K} s_m}{1 + \mathscr{K}^2} \quad \text{and} \quad \mathscr{L}_*^{-1} s_m = \frac{-\mathscr{K} c_m + s_m}{1 + \mathscr{K}^2} \tag{5.3}$$

in which $\mathscr{K} = m(R - (m^2 - 1)\alpha)$. At each order $O(\gamma^k)$, a sweeping procedure similar to that employed in the time-dependent case is used to construct particular integrals efficiently: CPU times required for fully automated solution of the order $O(\gamma^k)$ problem are 0.03, 0.06, 0.21, 1.28, 3.36, 19.57 and 119.6 s for $k = 1, \ldots, 7$. Clearly, h_1^* and h_2^* are, respectively, given by the time-independent components of h_1 and h_2 in (3.5) and (3.8), but h_k^* for $k = 3, \ldots, 7$ (too cumbersome to present) could not similarly have been obtained as $h_k^* = \lim_{t \to \infty} h_k$ without an astronomical increase in cost and effort. The first three terms in the perturbed flux are

$$\mathscr{Q}_N = 1 - \frac{3}{2(1 + R^2)}\gamma^2 + \frac{24R^4 - 144R^3\alpha + \left(216\alpha^2 + 273\right)R^2 - 792R\alpha + 216\alpha^2 - 75}{8\,(1 + R^2)^3(1 + 4(R - 3\alpha)^2)}\gamma^4. \tag{5.4}$$

Comparison with previous work on the steady state is facilitated by using the rescaled dependent variable and parameters

$$\eta = \frac{\mathscr{H}}{\mathscr{Q}}, \quad \beta = \gamma \mathscr{Q}^2, \quad \delta = \alpha \mathscr{Q}^3 \quad \text{and} \quad \lambda = R\mathscr{Q}^3, \tag{5.5}$$

to transform (5.1) into an ordinary differential equation for $\eta(\theta)$,

$$\frac{\eta - 1}{\eta^3} = \beta \cos\theta - \delta(\eta_\theta + \eta_{\theta\theta\theta}) - \lambda\eta_\theta, \tag{5.6}$$

in which $\eta(\theta) = \eta(\theta + 2\pi)$. When $\delta = \lambda = 0$ (5.6) is an algebraic equation for which Moffatt (1977) finds a solution η that is symmetric about, and achieves a maximum value at, $\theta = 0$. A series solution of $\partial_\theta \mathscr{H}_N^* = 0$ reveals that surface tension and inertia displace the maximum to

$$\theta \approx \gamma \tan^{-1} R + \frac{9(R - 2\alpha)\gamma^2}{(1 + R^2)(1 + 4(R - 3\alpha)^2)} + O(\gamma^3), \tag{5.7}$$

in which it should be remembered from § 4 that a steady state requires $R < R_0$, where R_0 is given by (4.6). When $R = \zeta R_0$ for $0 < \zeta < 1$ (5.7) gives

$$\theta_0 \approx -\frac{18\alpha\gamma}{1 + 36\alpha^2} + O(\zeta\alpha\gamma^2), \tag{5.8}$$

and so the maximum is displaced downwards for all $0 < R < R_0$ and $\alpha > 0$; this is confirmed by numerical integrations of (5.1). Figure 7 shows curves in (β, η) space computed using (5.1), (5.4) and (5.5), with η calculated at both $\theta = 0$ and $\theta = \theta_0$, for a range of values of α. The largest value of γ used in parameterizing all curves in figure 7 is dictated by Moffatt's maximum-load criterion when $\alpha = 0$, in which case the critical value of $\gamma \approx 0.16665470713578132360$ has been obtained exactly in terms of elliptic integrals by Metcalfe (2005, private communication). As a curiosity, it reveals that the maximum load differs from $\pi\sqrt{2}$ by only 3.6×10^{-3} %. As N is increased, the small-α solutions converge on the solution curve of Moffatt (1977).

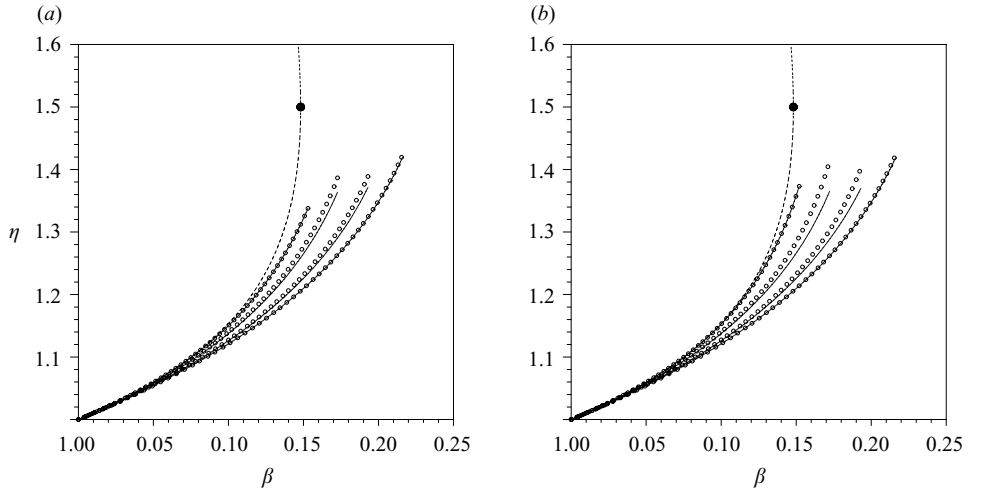

FIGURE 7. Variations in $\eta_N(\theta)$ and β_N for (*a*) $N=4$ and (*b*) $N=6$ at $\theta=0$ (solid lines) and $\theta=\theta_0$ (circles). From left to right along the β-axis, pairs of curves correspond to $\alpha=0.001$, 0.1, 0.3 and 10.0 in $\mathscr{H}_N^*$, parameterized by γ taking maximum values of γ of 0.17, 0.20, 0.23 and 0.26, respectively. Solid lines and circles have $R=0$ and $R=R_0$, respectively. The left-most dashed curve corresponds to the cubic equation $\beta\eta^3+\eta-1=0$ for the $\alpha=0$ solution at $\theta=0$ obtained by Moffatt (1977); the black disc at $(4/27, 3/2)$ on this curve corresponds to the maximum-load solution.

Let $\eta_0=\eta(0)$, in which $R=0$, and let $\eta_{R_0}=\eta(\theta_0)$, in which $R=\zeta R_0$ $(0<\zeta<1)$, and define $\Delta\eta\equiv\eta_{R_0}-\eta_0$. The two notable features of figure 7 are that $\Delta\eta>0$ and that, apparently, $\Delta\eta\to0$ as $\alpha\to0$ and $\alpha\to\infty$. From (5.1), (5.5) and (5.8), it is straightforward to show that

$$\Delta\eta=\frac{162\alpha^2\gamma^3}{(1+36\alpha^2)^2}+O(\zeta\alpha^2\gamma^4),$$

which not only explains all features illustrated in figure 7, but also reveals that $\Delta\eta$ is maximized when $\alpha=1/6$; note that $\Delta\eta$ is visible in figure 7 for those curves whose α is close to this value. At this value of α, θ_0 attains its minimum of $-(3/2)\gamma$, thereafter increasing back to 0 as $\alpha\to\infty$, which limit is now discussed.

Via numerical integral-equation solutions of the full Stokes-flow problem, Hansen & Kelmanson (1994) discovered that the free-surface elevation is only weakly dependent on α as it varies over two decades in magnitude. Hinch & Kelmanson (2003) similarly show that their asymptotic solution (corresponding to) $\mathscr{H}_N(\theta,t)$ is insensitive to large variations in α, even those violating the hierarchy (2.39). By both studies, the limit $\alpha\gg1$, equivalently $\delta\gg1$, is physically plausible. In this limit, the leading-order small-γ approximation to R_0 given by (4.7), $\widetilde{R}_0\approx81\alpha\gamma^2/(1+144\alpha^2)$, assumes a maximum value of $27\gamma^2/(8+111\gamma^2)$ (with a maximum of $9/37\approx0.243$) at $\alpha=1/12$, decreasing thereafter according to the new critical value

$$\widetilde{R}_\infty=\frac{9\gamma^2}{4(4-3\gamma^2)\alpha}+O(\alpha^{-2}),\quad 0<\gamma\ll1,\quad \alpha\to\infty. \tag{5.9}$$

The implication of (5.9) is that a stable solution requires the reduction of inertia as surface tension increases without limit: this opposes the intuitive notion that increasing surface tension should stabilize increasing inertial effects. However (5.9) is

both corroborated by numerical integration of the time-dependent evolution equation (2.36) and consistent with the following argument.

As $\delta \to \infty$ (5.6) can have 2π-periodic solutions via two possible dominant balances. The first balance, $\lambda \ll \delta$, yields solutions of the form $\eta = a + b\cos\theta + c\sin\theta$ for some constants $\{a, b, c\}$; by (5.5) and the fact that $\mathscr{Q} = 1 + O(\gamma^2)$, this balance is compatible with (5.9). The second balance, $\lambda \approx \delta$, yields solutions of the form $\eta = a + b\cos n\theta + c\sin n\theta$ provided that $1 + \lambda/\delta = n^2$ for some $n \in \mathbb{N}$. This is equivalently $\lambda = (n^2 - 1)\delta$ or, by (5.5),

$$R = (n^2 - 1)\alpha, \quad n \in \mathbb{N}, \quad \alpha \to \infty. \tag{5.10}$$

Since (5.10) violates (5.9), the second balance is rejected, and this moreover ensures that the potentially singular terms in (4.2) remain bounded in the time-dependent solution. An independent mathematical observation yet to emerge further corroborates rejection of (5.10).

Substituting $R = \zeta R_\infty$, $0 < \zeta < 1$, into $\eta_\infty \equiv \mathscr{H}_6^*/\mathscr{Q}_6^*$ and letting $\alpha \to \infty$ gives, after expanding in powers of $\gamma \ll 1$,

$$\begin{aligned}\eta_\infty = {} & 1 + \tfrac{3}{2}\gamma^2 + \tfrac{3}{2}\gamma^4 + \left(\gamma + \tfrac{3}{2}\gamma^3 + \tfrac{9}{8}\gamma^5\right)\cos\theta \\ & + \alpha^{-1}\left\{\left(\left(\tfrac{9}{16}\zeta - \tfrac{3}{4}\right)\gamma^3 + \left(\tfrac{81}{64}\zeta - \tfrac{61}{32}\right)\gamma^5\right)\sin\theta\right. \\ & - \left(\tfrac{1}{4}\gamma^2 + \tfrac{11}{24}\gamma^4\right)\sin 2\theta + \left(\tfrac{1}{16}\gamma^3 + \tfrac{17}{128}\gamma^5\right)\sin 3\theta \\ & \left. - \tfrac{1}{48}\gamma^4 \sin 4\theta + \tfrac{1}{128}\gamma^5 \sin 5\theta\right\} + O(\alpha^{-1}\gamma^6, \alpha^{-2}),\end{aligned} \tag{5.11}$$

which is presented in detail to highlight several features. First, inertial terms, signified by ζ, exert minimal influence in this limit. Second, the first harmonic $\sin 2\theta$ unexpectedly has a much larger coefficient than the fundamental mode $\sin\theta$, whose coefficient is of the same order as the second harmonic $\sin 3\theta$. Third, in accord with the bounds in Pukhnachov (2005*a*), the constant term is greater than unity, the coefficient of $\cos\theta$ is positive, and the coefficient of $\sin\theta$ is always negative (here, because $0 < \zeta < 1$).

Equation (5.11) could in theory alternatively be obtained by a perturbation of the analysis in Pukhnachov (2005*a*, *b*) and Karabut (2007), in which

$$\eta_\infty = s + q\cos\theta - r\sin\theta, \quad \delta \to \infty, \tag{5.12}$$

where $s > 1$ and $q, r \geqslant 0$ (see above). Since by (5.12) s is the mean value of η_∞ in $0 \leqslant \theta \leqslant 2\pi$, and since it is now known from (5.8) that the maximum value of η returns to $\theta = 0$ as $\delta \to \infty$, it is also the case that the mean value of η returns to $\theta = \pi/2$, hence $s \equiv \eta_\infty(\pi/2)$ in (5.12). In Pukhnachov (2005*a*) (5.12) is inserted into (5.6), with $\lambda = 0$, and both sides multiplied by the three basis functions $\{1, \cos\theta, \sin\theta\}$ and integrated from $\theta = 0$ to $\theta = 2\pi$ via residue theory to yield (after division by π throughout) three nonlinear equations in s, q and r, which can be expressed in the form

$$s(3s - 2\mathscr{T}) = \mathscr{T}, \tag{5.13}$$

$$q(3s - 2\mathscr{T}) = (\beta + \lambda r)\mathscr{T}^{5/2}, \tag{5.14}$$

$$r(3s - 2\mathscr{T}) = -\lambda q\mathscr{T}^{5/2}, \tag{5.15}$$

in which $\mathscr{T} = s^2 - q^2 - r^2$. When $\lambda = 0$, (5.13)–(5.15) admit a semi-explicit solution: first, $r = 0$ from (5.15), whence (5.13) gives $q = q(s)$ explicitly, then (5.14) yields the

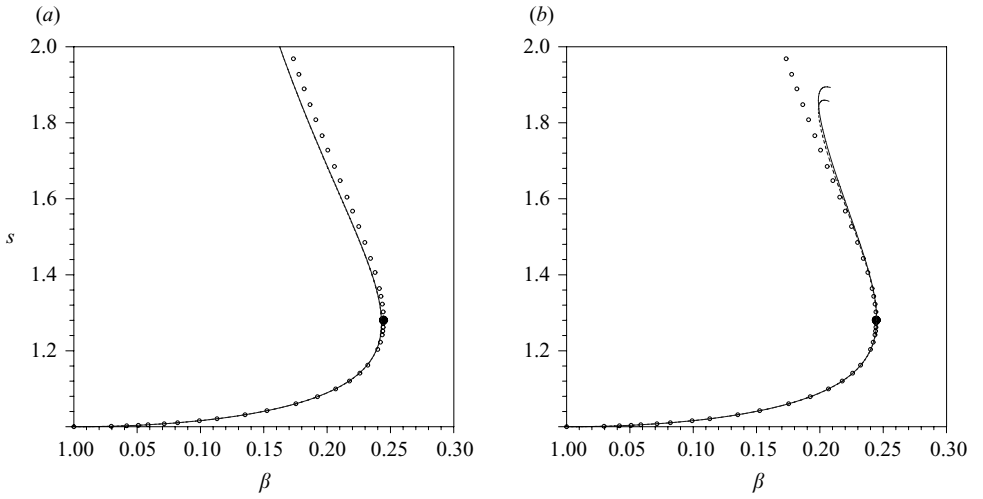

FIGURE 8. Large-α variations in $s_N = \eta_{\infty_N}(\pi/2)$ and β_N when $R = R_\infty$, (*a*) $N = 4$ and (*b*) $N = 6$. $\mathscr{H}^*_N$, parameterized by $0 \leqslant \gamma \leqslant 0.75$, is shown for $\alpha = 10$ (dashed line) and $\alpha = 100$ (solid line). The small circles describe the sextic curve (5.16) of Pukhnachov (2005*a*), on which the black disc at the critical point $((1/24)(17^{3/2} - 107/3)^{1/2}, (1 + \sqrt{17})/4)$ signifies the point below which exist thin-film solutions of the type presently studied, and above which large surface tension stabilizes static pendant drops. The present theory deviates notably from the theoretical curve, particularly as N is increased, when larger values of γ are used. As $\alpha \to \infty$, $\gamma \approx 0.4$ at the critical point.

following sextic equation,

$$27\beta^2 s^6 - 8s^3 + 6s + 2 = 0, \tag{5.16}$$

which has to be solved implicitly for s either asymptotically in the small-β limit, as in Pukhnachov (2005*a*), or numerically for larger values, as in Karabut (2007). For sufficiently small β there are two real values of s, one of which corresponds to the thin film analysed in §§ 3 and 4. The other corresponds to a large pendant drop. Note here that, if the alternative $\eta_\infty = a + b\cos n\theta + c\sin n\theta$ $(n > 1)$ associated with (5.10) is used, the right-hand sides of both (5.14) and (5.15) vanish for all λ, b and c, thereby making the solution independent of β and λ. This is the final reason for rejecting (5.10).

By (5.9), when $\lambda > 0$ it is given by the rescaling (5.5) as

$$\lambda = \frac{9\beta^2 \mathscr{Q}^6}{4(4\mathscr{Q}^4 - 3\beta^2)\delta} \ll 1,$$

in which case it may be possible to use the exact solution at leading-order to solve (5.13)–(5.15) using large-δ asymptotics. However, this is eschewed since an asymptotically correct solution (5.11) has been obtained explicitly, and this solution has already revealed that the contribution from the inertial perturbation is negligible in this limit. Figure 8 shows a comparison in the (β, s) plane between s computed from (5.11), for large α, and that predicted by (5.16), for $\alpha \to \infty$: the most striking feature is that (5.11), derived from the thin-film approximation, appears to predict accurate values of s beyond the critical value of β, well into the pendant-drop régime, in which γ becomes order $O(1)$. However, this implies that only $\mathscr{H}^*_N(\pi/2)$ is accurately

estimated for $\gamma = O(1)$, and further calculations reveal that $\mathscr{H}_N^*(\theta)$ in this régime is not uniformly well represented in $0 \leqslant \theta \leqslant 2\pi$.

In conclusion, inertia fundamentally changes the nature of the exterior MPP because without it the steady state is reached for all $\gamma \ll 1$ and, in practice, several decades of α. Once inertia is introduced, certain $\{\gamma, \alpha, R\}$ balances preclude the existence of a steady state even though a steady-state analysis does not reveal this. Indeed, the steady-state profile is known to be insensitive to variations in R, yet the critical Reynolds number R_0 (and, by association, R_∞) through which it can be reached is bounded with increasing severity as surface tension is increased. Accordingly, it remains an open and interesting question as to whether or not such bounds can be determined directly from an analysis of the steady-state problem, without having to negotiate the more difficult and indirect path of a multiple-timescale analysis of the full evolutionary problem.

It is also interesting to speculate whether or not the $R = O(\alpha\gamma^2)$ balance discovered in the evolutionary problem corresponds to the thin-film MPP whilst the $R = O(\alpha)$ balance of (5.10) – which does arise naturally in the steady-state analysis – corresponds only to the pendant-drop MPP. In that case, the problem of the potential singularities of § 3 may be resurrected in a time-dependent thick-film solution of the exterior MPP.

REFERENCES

Acrivos, A. & Jin, B. 2004 Rimming flows within a rotating horizontal cylinder: asymptotic analysis of the thin-film lubrication equations and stability of their solutions. *J. Engng Math.* **50**, 99–120.

Ashmore, J., Hosoi, A. E. & Stone, H. A. 2003 The effect of surface tension on rimming flows in a partially filled rotating cylinder. *J. Fluid Mech.* **479**, 65–98.

Benilov, E. S. & O'Brien, S. B. G. 2005 Inertial instability of a liquid film inside a rotating horizontal cylinder. *Phys. Fluids* **17**, 1–16.

Benjamin, T. B., Pritchard, W. G. & Tavener, S. J. 1993 Steady and unsteady flows of a highly viscous liquid inside a rotating horizontal cylinder. Report No. AM 122. Department of Mathematics, Penn State University.

Brandrup, J., Immergut, E. H., Bloch, D. R. & Grulke, E. A. (Eds.) 2003 *The Polymer Handbook*, 4th ed., Wiley.

Evans, P. L., Schwarz, L. W. & Roy, R. V. 2004 Steady and unsteady solutions for coating flow on a rotating horizontal cylinder: two-dimensional theoretical and numerical modelling. *Phys. Fluids* **16**, 2742–2756.

Hansen, E. B. & Kelmanson, M. A. 1994 Steady, viscous, free-surface flow on a rotating cylinder. *J. Fluid Mech.* **272**, 91–107.

Hinch, E. J. & Kelmanson, M. A. 2003 On the decay and drift of free-surface perturbations in viscous, thin-film flow exterior to a rotating cylinder. *Proc. Roy. Soc. Lond.* A **459**, 1193–1213.

Hinch, E. J., Kelmanson, M. A. & Metcalfe, P. D. 2004 Shock-like free-surface perturbations in low-surface-tension, viscous, thin-film flow exterior to a rotating cylinder. *Proc. Roy. Soc. Lond.* A **460**, 2975–2991.

Hocking, L. M. & Davis, S. H. 2002 Inertial effects in time-dependent motion of thin films and drops. *J. Fluid Mech.* **467**, 1–17.

Hosoi, A. E. & Mahadevan, L. 1999 Axial instability of a free-surface front in a partially filled horizontal rotating cylinder. *Phys. Fluids* **11**, 97–106.

Karabut, E. A. 2007 Two régimes of liquid film flow on a rotating cylinder. *J. Appl. Mech. Tech. Phys.* **48** (1), 55–64.

Kelmanson, M. A. 1995 Theoretical and experimental analyses of the maximum-supportable fluid load on a rotating cylinder. *J. Engng Math.*, **29** (3), 271–285.

KELMANSON, M. A. 2009 Pseudo-three-timescale approximation of exponentially modulated free-surface waves, *J. Fluid Mech.* **625**, 435–443.

KEVORKIAN, J. & COLE, J. D. 1996 *Multiple Scale and Singular Perturbation Methods*. Springer-Verlag.

MOFFATT, H. K. 1977 Behaviour of a viscous film on the outer surface of a rotating cylinder. *J. Méc.* **187**, 651–673.

MURDOCK, J. A. 1991 *Perturbations: Theory and Methods*. SIAM, Wiley.

NOAKES, C. J., KING, J. R. & RILEY, D. S. 2006 On the development of rational approximations incorporating inertial effects in coating and rimming flows: a multiple-scales approach. *Q. J. Mech. Appl. Math.* **59**, 163–190.

PETERSON, R. C., JIMACK, P. K. & KELMANSON, M. A. 2001 On the stability of viscous free-surface flow supported by a rotating cylinder. *Proc. Roy. Soc. Lond.* A **457**, 1427–1445.

PUKHNACHEV, V. V. 1977 Motion of a liquid film on the surface of a rotating cylinder in a gravitational field. *J. Appl. Mech. Tech. Phys.* **18**, 344–351.

PUKHNACHOV, V. V. 2005*a* On the equation of a rotating film. *Siber. Math. J.* **46** (5), 913–924.

PUKHNACHOV, V. V. 2005*b* Capillary/gravity film flows on the surface of a rotating cylinder. *J. Math. Sci.* **130** (4), 4871–4883.

WILSON, S. K., HUNT, R. & DUFFY, B. R. 2002 On the critical solutions in coating and rimming flow in a uniformly rotating horizontal cylinder *Q. J. Mech. Appl. Math.* **55**, 357–383.